J Neurophysiol 91: 449–473, 2004.
First published September 10, 2003; 10.1152/jn.00876.2002.

Neuronal Activity in the Supplementary Motor Area of Monkeys Adapting to a New Dynamic Environment

Camillo Padoa-Schioppa, Chiang-Shan Ray Li, and Emilio Bizzi
McGovern Institute for Brain Research, Department of Brain and Cognitive Sciences, Massachusetts Institute of Technology, Cambridge, Massachusetts 02139

Submitted 1 October 2002; accepted in final form 4 September 2003

Padoa-Schioppa, Camillo, Chiang-Shan Ray Li, and Emilio Bizzi. Neuronal activity in the supplementary motor area of monkeys adapting to a new dynamic environment. *J Neurophysiol* 91: 449–473, 2004. First published September 10, 2003; 10.1152/jn.00876.2002. To execute visually guided reaching movements, the central nervous system (CNS) must transform a desired hand trajectory (kinematics) into appropriate muscle-related commands (dynamics). It has been suggested that the CNS might face this challenging computation by using internal forward models for the dynamics. Previous work in humans found that new internal models can be acquired through experience. In a series of studies in monkeys, we investigated how neurons in the motor areas of the frontal lobe reflect the movement dynamics and how their activity changes when monkeys learn a new internal model. Here we describe the results for the supplementary motor area (SMA-proper, or SMA). In the experiments, monkeys executed visually guided reaching movements and adapted to an external perturbing force field. The experimental design allowed dissociating the neuronal activity related to movement dynamics from that related to movement kinematics. It also allowed dissociating the changes related to motor learning from the activity related to motor performance (kinematics and dynamics). We show that neurons in SMA reflect the movement dynamics individually and as a population, and that their activity undergoes a variety of plastic changes when monkeys adapt to a new dynamic environment.

INTRODUCTION

The mechanics of movements is described at two different levels: the dynamics and the kinematics. For a reaching movement, the dynamics describes the forces—exerted by contracting muscles—that cause the movement [$f(t)$]. The kinematics describes the position of the hand and the joint angles in time [$x(t)$], together with the time derivatives [$\dot{x}(t)$ and $\ddot{x}(t)$]. The mechanics of movements is described by Newton's equation, which relates the dynamics and the kinematics. For planning and executing visually guided reaching movements, it is widely assumed that the CNS undertakes a sequence of operations, which can be grouped in *1*) processing of the visual stimuli (including all stages "upstream" of the kinematics, such as making the decision to reach), *2*) designing the desired kinematics, and *3*) computing the corresponding desired dynamics (Alexander and Crutcher 1990a; Bernstein 1967; Kalaska and Crammond 1992; Mussa-Ivaldi and Bizzi 2000; Saltzman 1979). Two fundamental issues remain open. First, what kinematic and dynamic variables are exactly coded? For instance, the endpoint, the total movement time, and the curvature of the trajectories are all valid kinematic variables. Likewise, the total force at the endpoint of the limb or the joint torques are valid dynamic variables. Second, how are these variables processed in the CNS? The present work investigated aspects of this second issue. Specifically, we investigated how the activity of neurons in the motor areas of the frontal lobe reflects the dynamics of movements.

Several investigators have proposed that the CNS processes the movement dynamics by the use of internal models, which describe the dynamics of the limb and the environment (Merfeld et al. 1999; Shadmehr and Mussa-Ivaldi 1994; Wolpert et al. 1995; for review see Desmurget and Grafton 2000; Kawato 1999; Wolpert and Ghahramani 2000). Work in humans and monkeys showed that new internal models can be acquired when subjects adapt to perturbing forces (Shadmehr and Mussa-Ivaldi 1994). In addition, new internal models for the dynamics allow some generalization (Gandolfo et al. 2000; Thoroughman and Shadmehr 2000) and undergo consolidation in the few hours after training (Brashers-Krug et al. 1996). Finally, internal models for the dynamics are learned independently of other internal models [e.g., internal models for the kinematics (Flanagan et al. 1999; Krakauer et al. 1999)]. In the present report, we describe how the activity of neurons in the supplementary motor area (SMA) reflects the internal model of the dynamics and how it is modified when a new internal model is acquired.

Investigation of the physiological underpinnings of movement dynamics has traditionally focused most extensively on the primary motor cortex (M1). Starting with Evarts (1968), many researchers found that neurons in M1 are modulated by external loads. This interest in M1 partly reflected a serial view of the motor systems. According to this view, several "premotor" areas process high sensorimotor processes and feed M1, which then projects to the spinal cord. More recently, however, it was found that direct corticospinal projections originate from multiple motor areas, including the SMA, the dorsal and ventral premotor areas, and the cingulate motor areas, in addition to M1 (He et al. 1993, 1995). These same areas are also intensely interconnected with each other (Luppino et al. 1990, 1993). Based on these findings and on the observation of often extensive functional overlap between different motor areas (Alexander and Crutcher 1990a,b; Crutcher and Alexander 1990; Scott and Kalaska 1997; Scott et al. 1997), it was proposed that different motor areas provide parallel contributions to the control of movements (Dum and Strick 1991; Prut and Fetz 1999). More specifically, corticospinal projections originating from multiple areas led us to hypothesize that

Address for reprint requests and other correspondence: C. Padoa-Schioppa, Department of Neurobiology, Harvard Medical School, 200 Longwood Ave., Room WAB 224, Boston, MA 02115 (E-mail: camillo@alum.mit.edu).

The costs of publication of this article were defrayed in part by the payment of page charges. The article must therefore be hereby marked "*advertisement*" in accordance with 18 U.S.C. Section 1734 solely to indicate this fact.

multiple areas might contribute to the processing of the movement dynamics. The present experiments were conducted to test this hypothesis with respect to the SMA.

Our experiments focused on SMA (or SMA-proper, or F3), which constitutes the caudal portion of the traditionally defined "*SMA*" (Penfield and Welch 1951; Woolsey et al. 1952), and which we distinguished from the more rostral preSMA (or F6). Converging evidence from anatomy and microstimulation work in monkeys and from imaging studies in humans strongly indicates a more direct involvement of SMA in movement planning and execution, whereas preSMA seems involved in more complex tasks (Bates and Goldman-Rakic 1993; He et al. 1995; Luppino et al. 1990, 1991, 1993, 1994; Matelli et al. 1991; Rouiller et al. 1996; see review by Geyer et al. 2000; imaging work reviewed by Picard and Strick 1996). Indeed, Picard and Strick (2001) note that "the connectivity and physiology of the preSMA suggest that it is more like a prefrontal area than a premotor area." We focused our experiments on SMA because we expected it more likely to find neuronal correlates of the movement dynamics—a late motor processing stage—in a properly "motor" area, closer to the motor output.

Unfortunately, most of the previous single-cell recordings in monkeys did not distinguish between preSMA and SMA. Neurons in "*SMA*" were investigated for their relation to complex motor functions (Chen and Wise 1995; Kurata and Tanji 1985; Mushiake et al. 1991; Okano and Tanji 1987; Tanji and Kurata 1985; Tanji et al. 1980; Thaler et al. 1995). More recently, however, Matsuzaka et al. (1992; Matsuzaka and Tanji 1996) revisited previous experiments on the instruction dependency of neuronal activity in "*SMA*." They found that the phenomenon was relatively common in preSMA, but negligible in SMA. Their work also showed that neurons in SMA often responded to somatosensory stimulation. Phasic, movement-related activity was more frequent in SMA, and its onset was often time locked with the movement onset. In contrast, responses to visual cues were more abundant in preSMA. Along a similar vein, Hikosaka and coworkers concluded after a series of studies in humans and monkeys that SMA is more relevant for movement per se, and—with respect to motor learning—"works to acquire explicit skill" (Hikosaka et al. 2000; Nakamura et al. 1998). These results confirmed prior observations of Alexander and Crutcher (1990a,b). Although their study did not explicitly distinguish between preSMA and SMA, they analyzed the neuronal activity recorded in the medial wall relative to the rostrocaudal location of recording. They found that neurons with only preparatory activity—and not movement-related activity—were located mostly anterior to the gAS (alignment with the genu of the arcuate sulcus) (i.e., in preSMA). In contrast, neurons with only movement-related activity—and not preparatory activity—were generally located posterior to the gAS (i.e., in SMA). Neurons with both preparatory and movement-related activity were found in both areas (Alexander and Crutcher 1990a). Likewise, neurons with target-dependent activity were found almost exclusively rostral to the gAS (i.e., in preSMA), whereas the activity of neurons caudal to the gAS (i.e., in SMA) was limb-dependent (Alexander and Crutcher 1990b). In conclusion, single-cell recordings that distinguished between the two areas support the view that SMA is much more closely related to the motor output.

With respect to the difference between SMA and M1, two complementary aspects seem to emerge. On the one hand, SMA appears more involved in motor planning than M1 is. For instance, Alexander and Crutcher (1990a) found preparatory activity (during an instructed delay) in 55% of SMA neurons versus 37% of M1 neurons. Correspondingly, the "lead time" (i.e., time of neuronal discharge onset relative to movement onset) was significantly longer for SMA (47 ± 8 ms) than for M1 (23 ± 6 ms) (Crutcher and Alexander 1990). On the other hand, SMA also seems closely related to the implementation of movements. For instance, Matsuzaka et al. (1992) found that a majority of SMA neurons were "movement-locked." Likewise, Crutcher and Alexander (1990) found comparable activity in SMA and M1 during motor execution. A direct role of SMA in motor execution also emerges from the studies reviewed by Hikosaka et al. (2000).

With respect to the comparison between SMA and the other "premotor" areas, few studies have thoroughly investigated this issue. However, Halsband and coworkers analyzed the changes in activity during 5 time windows [instruction, delay, premovement, movement, and reward (Halsband et al. 1994)]. They found substantially similar percentages in SMA and in the (combined) PMd and PMv. Cadoret and Smith (1997) found similar activation in SMA and in the ventral cingulate motor area in a prehension task.

Dynamics-related activity of neurons in SMA was previously investigated by Alexander and Crutcher. With respect to the activity *during motor execution*, they found dynamics-related signals in comparable proportions in SMA and in M1 (41% of "muscle-like" cells in SMA versus 36% in M1) (Crutcher and Alexander 1990). With respect to the activity *during motor planning*, they found that 18% of SMA cells were "muscle-like" (Alexander and Crutcher 1990b). Thus, dynamics-related activity was present in SMA also during planning, although in smaller proportion. (Although the authors concluded that the dynamics-related signal was "nearly absent," with a criterion threshold of $P < 0.001$, the measure of 18% is quite significant.) In the present study, we confirm and strengthen these results by showing that the movement dynamics is significantly present at the level of the population in SMA both during motor planning and during motor execution. In addition, we show that neurons in SMA undergo a variety of plastic changes when a new internal model for the dynamics is acquired. These plastic changes are comparable to that found in M1 (Gandolfo et al. 2000; Li et al. 2001). Parts of this work were presented elsewhere (Padoa-Schioppa et al. 2000, 2002).

METHODS

The experimental setup, behavioral paradigm, and data analysis were the same used for a previous study of M1 (Li et al. 2001) except when otherwise specified. The National Institutes of Health guidelines on the care and use of animals were strictly followed throughout the experiment.

Behavioral task

Two young male rhesus monkeys (*Macaca mulatta*), C and F, took part in the experiment. Both monkeys weighed between 6.5 and 7.5 kg, and both performed with the right arm. In the experiment, the monkeys sat on a chair in an electrically isolated enclosure. They held the handle of a 2 degrees of freedom (*df*) robotic arm (the manipulandum), which allowed free movements confined to a horizontal

plane. A computer monitor placed vertically 75 cm in front of the monkeys displayed the position of the handle (cursor: 3 × 3-mm square, 0.2° of visual angle) and the targets of the reaching movements (16 × 16-mm squares, 1° of visual angle). All the movements were from a central location (center square) to one of 8 peripheral targets (peripheral squares), equally spaced along a circle (45° apart). Actual reaching movements were 8 cm in length.

The monkeys performed an instructed delayed reaching task. At the beginning of each trial, the center square appeared on the monitor, and the monkey moved the cursor into the center square to initiate the trial. After 1 s, a target square appeared at one of the 8 peripheral locations (*cue*). The monkey held the cursor within the center square for a randomly variable delay (0.5–1.5 s) before the center square was extinguished (*go* signal). The monkey had then to move and acquire the peripheral square within 3 s, and to remain within the peripheral square for 1 s to receive a juice reward (*rew*). During the task, the trajectories had to be confined within 60° on both sides of the line passing through the center square and peripheral square. The trial was immediately aborted if the monkey made any error, and another trial started after an intertrial interval (*iti*) of 0.8–1.2 s. The peripheral targets were pseudo-randomly chosen.

Two motors attached at the base of the robotic arm allowed turning on and off perturbing forces (force fields). We used one of the 2 force fields described by $\mathbf{F} = \mathbf{BV}$, where $\mathbf{B}$ is the rotation matrix ($\mathbf{B} = [0, -b; b, 0]$, with $b = \pm 0.06$ N s cm^{-1}) and $\mathbf{V}$ is the instantaneous velocity vector. Thus the force field $\mathbf{F}$ was viscous (proportional in strength to the velocity $\mathbf{V}$) and curl (orthogonal in direction to the velocity $\mathbf{V}$). Depending on the sign of "b" the force field was clockwise (CK) or counterclockwise (CCK). In each session, the monkeys performed in 3 subsequent behavioral conditions: BASELINE (no force), FORCE, and WASHOUT (no force). Each condition lasted for about 20 successful trials for each direction (about 160 trials total). Only one of the 2 force fields (CK or CCK) was used in each session.

Monkeys were exposed only to the nonperturbed reaching task during the training (4–6 mo), and the force fields were introduced only during the recording sessions. For monkey C, recording sessions with the 2 force fields were run in blocks (27 sessions with the CK force field, followed by 28 sessions with the CCK force field). Monkey F was tested on the CCK force field only (40 sessions). Sometimes, recording sessions began after the monkey had performed in nonperturbed conditions for ≤300 trials, allowing the time for the electrodes to settle, and for us to accurately define the spike thresholds. Each recording session lasted 1–2 h, after which we let the monkeys work as long as they continued. We ran no more than one session per day.

On separate control sessions we followed the same procedure, without ever introducing the perturbing force field. Thus in control sessions, the monkey performed in 3 arbitrarily divided conditions of about 160 successful trials each. Control sessions were intermixed with experimental sessions across days (16 control sessions in total).

Surgery and identification of the recording area

Aseptic stereotaxic surgery was performed to put a restraint device on the skull and a recording well (inner diameter: 28 mm and 19 mm for monkeys C and F, respectively). The chambers were centered on the midline, and in anterior coordinates A = 22 and A = 18 for monkeys C and F, respectively. The monkeys were given antibiotics and pain medications, and were allowed to fully rest for 1 wk after the surgery.

SMA was identified through electrical microstimulation (monkey C) and histology (monkey F). For microstimulation, we used a train of 20 biphasic pulse pairs (width = 0.1 ms, duration = 60 ms), at 330 Hz and 10–40 μA. Before the recordings, we extensively stimulated the left medial wall and obtained a map closely matching previous reports (Luppino et al. 1991). Monkey F was killed at the end of the experiment. We marked the recording sites with electrolytic lesions (cathodal current, 20 μA, 2 min). We then administered an overdose of pentobarbital sodium, and perfused the monkey transcardially with heparinized saline, followed by buffered formalin. The brain was marked with electrodes dipped in black ink, removed from the skull, photographed, sectioned (coronal plane, 28-μm sections), and Nissl-stained. Recordings were located in the medial wall, caudal to the alignment with the genu of the arcuate sulcus (gAS). Microscopic inspection revealed that the recording region was poorly laminated, and lay within 6 mm rostral to tissue displaying a single line of giant pyramidal cells, thus identifying SMA (Matelli et al. 1991).

Recordings

For neuronal recordings, we used vinyl-coated tungsten electrodes (1–3 MΩ impedance). We advanced electrodes by manually rotating a threaded rod carrying the electrode in a set-screw system, at an approximate depth resolution of 30 μm (300 μm/turn). Up to 8 electrodes were used in each session. Electrical signals acquired by the electrodes passed through a head stage (AI 401, Axon Instruments) and an amplifier (Cyberamp 380, Axon Instruments), and were filtered at a high and low cutoff of 10 kHz and 300 Hz, respectively. Data from each electrode were recorded and displayed using commercially available software (Experimenter's WorkBench 5.3, DataWave Technology). Electrical signals from each electrode were continuously sampled at a frequency of 20 kHz. Action potentials were detected by threshold crossing. Their waveforms (1.75-ms duration) were recorded on-line and saved to disk for subsequent analysis.

Data analysis: psychophysics

From each trajectory $\mathbf{x}(t) = [x(t), y(t)]$, we computed the speed profile $\mathbf{s}(t) = \|\mathbf{x}(t)\|$. Thus $\mathbf{s}(t)$ was a vector of instantaneous speeds, sampled at 100 Hz. We defined the movement onset (*mo*) and movement end (*me*) with a threshold-crossing criterion on the speed (4 cm/s). We also defined the following positions. The initial position (IP) was the average hand position in the 50 ms preceding the *mo*. The movement position (MP) was the weighted average of the hand position during the 500 ms after the *mo*, with exponentially decaying weights and time constant $\tau = 50$ ms. In formulaic expression

$$\mathrm{MP} = \int_{mo}^{mo+500} \mathbf{x}(t) e^{-t/\tau} dt \Big/ \int_{mo}^{mo+500} e^{-t/\tau} dt$$

The final position (FP) was the average hand position from the *me* to the delivery of the reward. We defined the perpendicular displacement as the distance between the hand trajectory computed at peak speed and the line passing through IP and FP. We defined the initial angular deviation d as the angle between the line passing through IP and MP and the line passing through IP and FP and so that $d > 0$ when movements deviated in the direction of the external force.

Following Shadmehr and Mussa-Ivaldi (1994), we defined the correlation coefficient (CC) as the normalized covariance between the actual speed profile and an ideal speed profile. We first derived an ideal speed profile $\mathbf{u}(t)$ with an iterative process as a corrected average of BASELINE speed profiles and separately for each session and for each movement direction. Then we aligned for each trial the actual speed profile $\mathbf{s}(t)$ with the corresponding ideal speed profile $\mathbf{u}(t)$ at their peaks, and we computed the correlation coefficient $\mathrm{CC}(\mathbf{s}, \mathbf{u}) = \mathrm{cov}(\mathbf{s}, \mathbf{u})/[\sigma(\mathbf{s})\sigma(\mathbf{u})]$. Hence, the values of the CC ranged between −1 and 1, and were close to 1 for actual speed profiles close to ideal.

To compare movements with similar kinematics, we disregarded for each condition the first 4 successful trials in each direction (32 successful trials in total). This arbitrary criterion was imposed for consistency with the previous work (Li et al. 2001; Padoa-Schioppa et al. 2002) and because it roughly corresponded to the initial adaptation phase. Loose time constraints were imposed on the reaction time (RT) during the experiments. In the analysis, we excluded anticipatory

movements (RT $<$ 200 ms) and outliers (RT $>$ 400 ms). The remaining trials ($>$88%) were considered for further analysis.

Data analysis: neurons

The neuronal recordings were first subjected to a clustering analysis, to separate one or more individual neurons recorded from the same electrode from each other and from noise. Clustering was performed using commercially available software (Autocut 3, DataWave Technology), with a semimanual procedure. We visually inspected the waveforms after clustering, and often repeated the procedure one or more times. Only cells with convincingly consistent waveform (i.e., stable recordings) throughout the session were considered for further analysis.

We analyzed the activity of single neurons in 4 separate time windows. The center hold time (CH; 500 ms before *cue*), serving as a control time window; the delay time (DT; 500 ms before *go*); the movement time (MT; from 200 ms before *mo* to *me*); the target hold time (TH; 500 ms before *rew*). For each neuron and for each time window, we analyzed the spiking activity separately in the BASELINE, FORCE, and WASHOUT conditions. We averaged the activity across trials, and obtained a tuning curve for each condition. To characterize the tuning curves, we defined 3 parameters: the preferred direction (Pd), the average firing frequency (Avf), and the tuning width (Tw). The Pd of the neuron was defined as the direction of the vector average of the 8 vectors representing the activity recorded for the 8 movement directions. The Avf was defined as the average of the neuronal activity across the 8 directions. The Tw was defined as the angle over which the firing frequency was higher than half of the maximal activity across the 8 directions (maximum of the tuning curve). These parameters were defined for any given tuning curve, subject to the following preconditions. First, we considered tuning curves only with Avf values $>$1 Hz. Second, the Pd and Tw were defined for tuning curves displaying only a significantly unimodal distribution across directions (a directional tuning), as stated by the Rayleigh test ($P < 0.01$; Fisher 1993). Third, the Tw was defined only for strictly unimodal cells, for which the directions with firing frequency higher than half the maximum were continuous.

To analyze the changes of Pd over the entire population, we "flipped" the data recorded with the CK force field to obtain positive values when the Pd shifted in the direction of the external force.

Classification of cells

Significant changes across conditions for the 3 parameters Pd, Avf, and Tw were stated according to the method previously described in detail (Li et al. 2001). Briefly, given the 8-dimensional firing rate $\vec{m}$, the 8-dimensional SE $\vec{\sigma}$ (due to trial-by-trial variability in the activity of the cell) can be thought of as an error of measure for $\vec{m}$. We can expand each parameter $p = P(\vec{m})$ at the first order in $\vec{m}$. Assuming that the 8 variables $\vec{m}$ are Gaussian, p is also Gaussian and σ_p can be estimated as a linear combination of the 8 errors $\vec{\sigma}$. For the analysis, we computed p and σ_p in each condition, and we compared the values of the parameter across conditions with a *z*-test ($P < 0.001$) using σ_p^2 as an estimate of the variance.

Individual cells were classified separately for each parameter (Pd, Avf, and Tw) and for each time window (CH, DT, MT, and TH). For the sake of clarity, we illustrate the criteria of classification referring to the Pd. Cells that did not change their Pd across conditions (*x*-*x*-*x*) were designated "kinematic cells" because the desired kinematics remained unchanged throughout the session (see RESULTS). Cells that changed their Pd in the FORCE condition compared with BASELINE and returned to the original Pd in the WASHOUT (*x*-*y*-*x*) were designated "dynamic cells" because the dynamics of the movement were the same in the BASELINE and in the WASHOUT but different in the FORCE condition (where the monkeys compensate for the external force). Cells that changed their Pd in the FORCE compared with the BASELINE, and maintained in the WASHOUT their newly acquired Pd (*x*-*y*-*y*) were designated "memory cells" because they appeared to keep trace of the adaptation experience even after the monkey had returned to the nonperturbed conditions. More precisely, *x*-*y*-*y* cells were designated "memory I cells," as distinguished from "memory II cells," whose Pd did not change in the FORCE condition compared with BASELINE, but changed in the WASHOUT compared with the FORCE condition (*x*-*x*-*y*). Thus memory II cells were complementary to memory I cells. Finally, cells that changed their Pd in the FORCE condition and again in the WASHOUT (*x*-*y*-*z*) were designated "other" cells. The same criteria were applied for the Avf and the Tw.

For the statistical analysis of the population, we used conventional methods of linear (Avf) and circular (Pd and Tw) statistics (Fisher 1993).

Comparing the results of different classifications

SMA cells were classified for their changes across behavioral conditions separately for the 4 time windows and 3 parameters. One of the goals of the present study was to compare the results of classification across time windows (CH, DT, MT, and TH), and across parameters (Pd, Avf, and Tw). In addition, we wanted to compare the results recorded for experimental cells with those recorded for control cells. Finally, we wanted to compare the results recorded here for SMA with those recorded from M1 (Gandolfo et al. 2000; Li et al. 2001). We performed these comparisons using a Pearson's χ^2 analysis (Freeman 1987), which we chose (over the likelihood ratio) because our contingency tables sometimes presented empty locations. For this same reason, we performed the comparison separately across populations, across time windows, and across parameters.

When comparing the classifications across time windows, we considered one parameter (e.g., the Avf) and 2 time windows (e.g., the DT and MT). We then addressed specific questions such as the following. Given that each given cell can be classified differently in the 2 time windows (e.g., "kinematic" in the DT and "dynamic" in the MT), are *coincident* classifications more frequent than would be expected if they occurred by chance? Having 5 possible classes (kinematic, dynamic, memory I, memory II, and other), we studied the 5×5 contingency table (5 DT classes $\times$ 5 MT classes) where the element n_{ij} is equal to the number of cells classified as "*i*" and "*j*" in the 2 time windows, respectively. We then computed the matrix

$$\chi^2_{ij} = \frac{(n_{ij} - m_{ij})^2}{m_{ij}}$$

where

$$m_{ij} = \frac{\sum_i n_{ij} \sum_j n_{ij}}{\sum_{i,j} n_{ij}}$$

Pearson's χ^2 is given by

$$\chi^2 = \sum_{i,j} \chi^2_{ij}$$

In essence, the matrix element χ^2_{ij} quantifies how "unlikely" is the value n_{ij} given all the other values n_{lk}, and χ^2 quantifies how "unlikely" is the table *n* if the distribution across rows is independent of the distribution across columns (and vice versa). In our case, χ^2 indicated whether the classifications in the DT and MT were at all interdependent, against the null hypothesis of homogeneity. To assess more specifically whether the 2 classifications coincided more frequently than expected by chance, we computed the trace

$$Tr = \sum_{i=j} \chi^2_{ij}$$

Because it is the sum of the diagonal elements of χ^2_{ij}, *Tr* precisely quantifies how unlikely are coincident classifications.

When comparing the classifications across parameters, we considered one time window (e.g., the MT) and 2 parameters (e.g., the Pd and the Avf). We then addressed specific questions such as the following. Given that each given cell can be classified differently for the 2 parameters (e.g., "dynamic" for the Pd and "memory I" for the Avf), are *coincident* classifications more frequent than would be expected if they occurred by chance? Again, we studied the 5×5 contingency table, which we analyzed like before. In particular, we computed both $\chi^2 = \Sigma_{i,j}\ \chi^2_{ij}$ and $Tr = \Sigma_{i=j}\ \chi^2_{ij}$.

A similar analysis was used when comparing the results for experimental and control cells. In this case, however, we collapsed cells of each group into 2 superclasses of "kinematic" and "nonkinematic" cells (nonkinematic cells included dynamics, memory I, memory II, and other cells). We obtained a 2×2 contingency table given by the 2 groups (experimental and control cells) and by the 2 superclasses (kinematics and nonkinematic cells). The value of Pearson's $\chi^2 = \Sigma_{i,j}\ \chi^2_{ij}$ indicated whether there were any differences between groups against the null hypothesis of homogeneity. Because kinematic cells were generally more frequent between control cells, a significant deviation from homogeneity always indicated a higher proportion of nonkinematic cells in the group of experimental cells than would be expected by chance.

Electromyographic activity

In separate sessions, we recorded the electromyographic (EMG) activity of the muscles pectoralis, deltoid, biceps, triceps, and brachioradialis while the monkey performed in the task. We manually implanted Teflon-insulated wires in the shoulder and arm muscles. The EMG were recorded continuously, at the frequency of 1 kHz. In the analysis, we rectified and integrated the EMG over the same time windows used for the neurons. We obtained EMG's tuning curves, which we normalized and submitted to the same analysis used for neurons.

RESULTS

Psychophysics

The psychophysics of the task was previously described for humans (Shadmehr and Mussa-Ivaldi 1994) and monkeys (Gandolfo et al. 2000; Li et al. 2001). The present study confirms and further documents those results. Figure 1 illustrates the hand paths and speed profiles recorded in a representative session. In the absence of external perturbation, hand paths were roughly straight (Fig. 1*A*, BASELINE) and the speed profiles were close to bell-shaped (Fig. 1*B*, BASELINE). When we introduced a CK force field (FORCE condition), the hand paths were initially deviated and the speed profiles were also perturbed (Fig. 1, *A* and *B*, EARLY FORCE). As the monkey adapted to the perturbing force, however, the paths and the speed profiles gradually recovered (Fig. 1, *A* and *B*, LATE FORCE). When we removed the force field, the trajectories were initially deviated in a way that mirrored the deviation observed in the EARLY FORCE. This "aftereffect" could be observed both in the hand paths and in the speed profiles (Fig. 1, *A* and *B*, EARLY

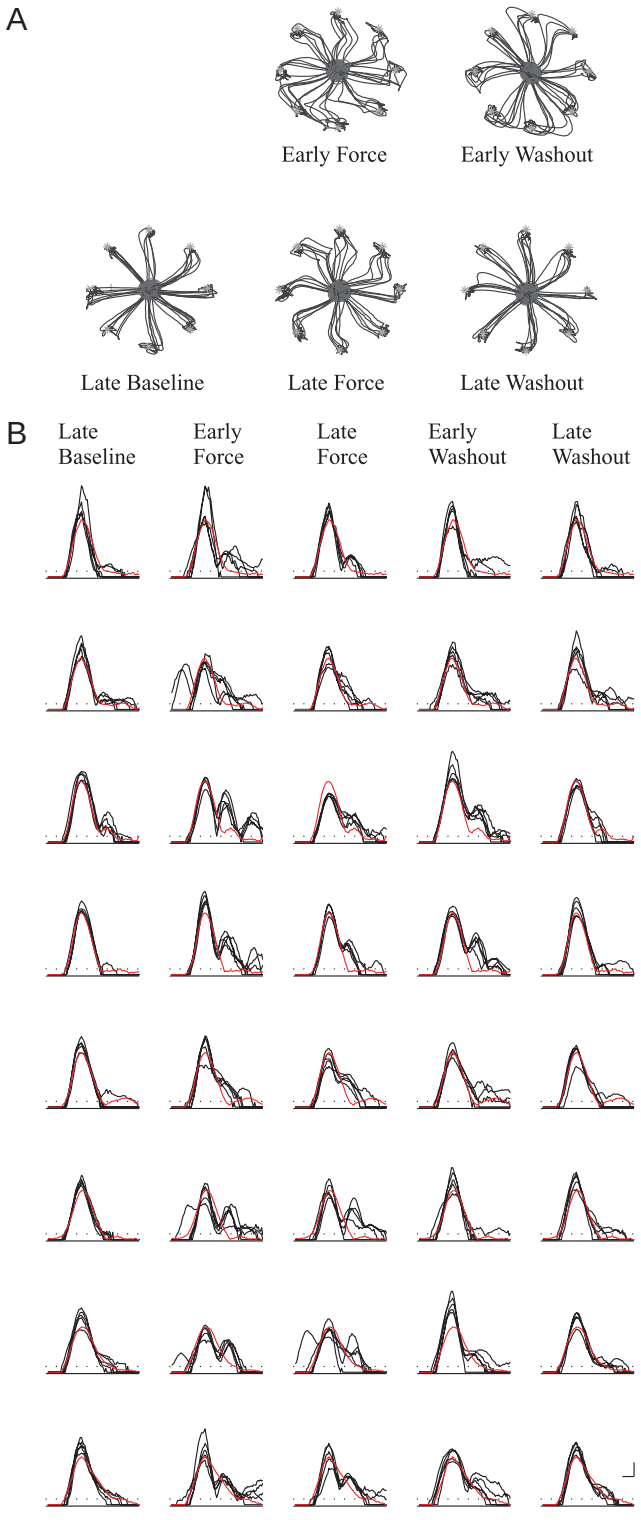

FIG. 1. Psychophysics of motor adaptation: hand paths and speed profiles. *A*: hand paths. Hand paths are initially straight (LATE BASELINE), and become deviated when a CK force field is introduced (EARLY FORCE). As the monkey adapts to the perturbation, however, the trajectories gradually return straight (LATE FORCE) and become similar to that observed in the BASELINE (adaptation, or short-term learning). A transient aftereffect can be observed when the force is removed (EARLY WASHOUT), when hand trajectories deviate in a way that mirrors that observed in the EARLY FORCE. However, the monkey rapidly readapts to the nonperturbed conditions, and the trajectories return straight (LATE WASHOUT). *B*: speed profiles. Speed profiles for the first/last 5 trials in each movement direction are shown for each condition. Movement directions are 1 to 8 (*top to bottom*). *Direction 1* is for rightward movements and direction number increases clockwise. Traces correspond to the hand trajectories illustrated in *A*, and the ideal speed profile is superimposed in red color. Dotted line indicates the threshold value of 4 cm/s. Unit bars on the bottom right represent 100 ms (x-axis) and 1 cm/s (y-axis).

WASHOUT), before the monkey readapted to the nonperturbed conditions (Fig. 1, *A* and *B*, LATE WASHOUT).

The adaptation process is well illustrated by the analysis of the perpendicular displacement of the hand path from the straight line connecting the initial position and the peripheral target (computed at peak speed) (Fig. 2*A*), and by the measure of the correlation coefficient (Fig. 2*B*). For example, it can be noticed that the correlation coefficient (CC) presents high values in the BASELINE; the CC drops initially in the FORCE condition, and gradually recovers as the monkey adapts; in the WASHOUT, the CC presents a brief aftereffect, before readaptation.

Adaptation improved over days (long-term learning), as observed through both the perpendicular displacement and the correlation coefficient. In Fig. 2*C*, we plotted the mean perpendicular displacement recorded in each session against the session number, separately for the 3 conditions BASELINE (black triangles), FORCE (blue circles), and WASHOUT (green inverted triangles). Over sessions, the mean perpendicular displacement recorded in the FORCE and in the WASHOUT conditions showed a convergence trend and gradually approached that recorded in the BASELINE. Analysis of the initial angular deviation over sessions provided very similar results (data not shown). Likewise, analysis of the mean correlation coefficient over sessions confirms this process of long-term learning (Fig. 2*D*).

Additional analysis indicates that other kinematic parame-

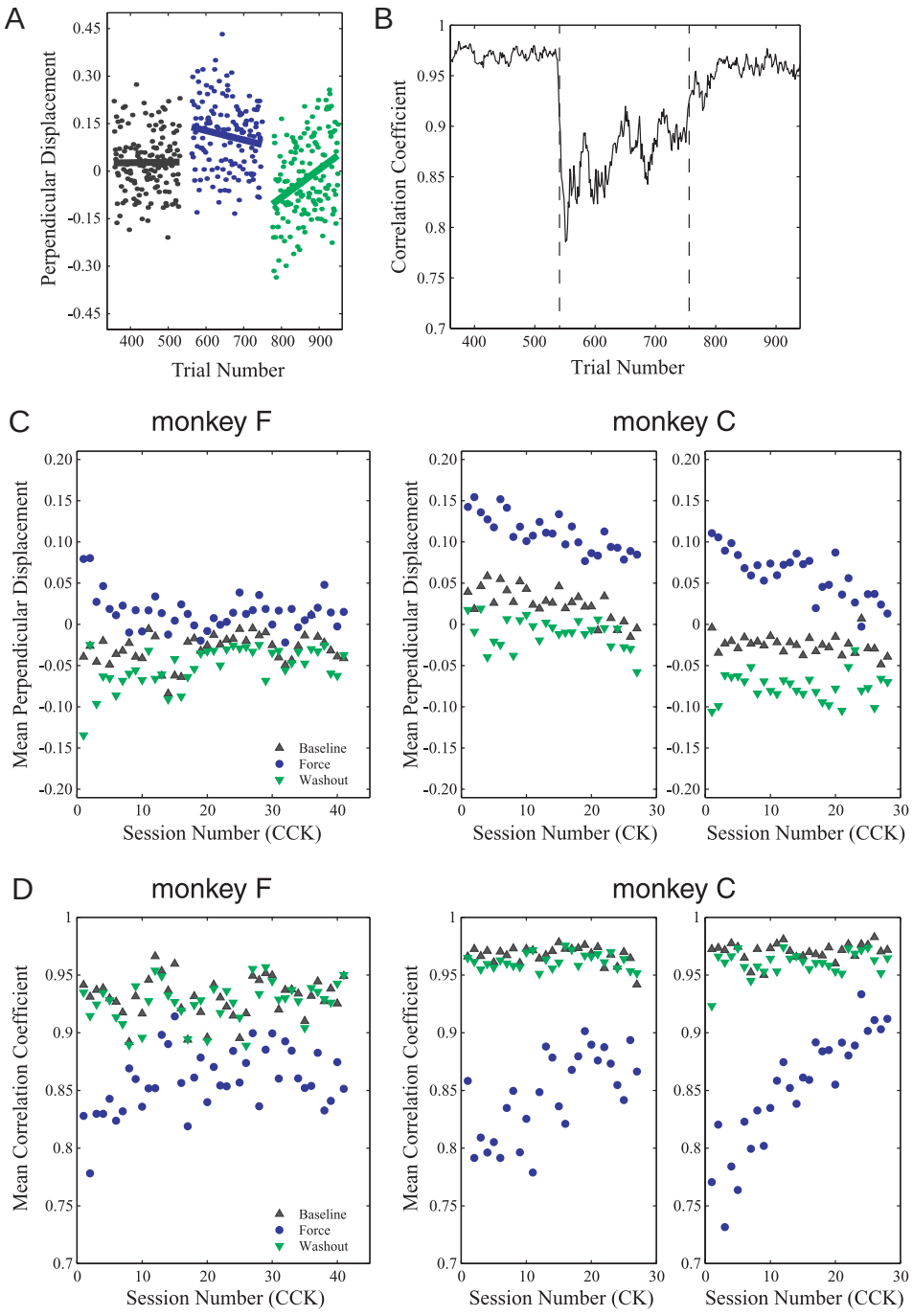

ters remained essentially constant across conditions. Figure 3, *A–C* illustrates, for each session, the measures of average peak speed, average reaction time, and average movement time. Quantitative analysis with a 2-way ANOVA (factors: monkey, condition) provided the following results. With respect to the peak speed, the main factor of condition was not significant ($F = 0.65$, $P > 0.5$) and the interaction factor was not significant ($F = 1.33$, $P > 0.2$). With respect to the average reaction time, the main factor of condition was not significant ($F = 0.01$, $P > 0.9$) and the interaction factor was not significant ($F = 0.6$, $P > 0.4$). Finally, with respect to the average movement time, the main factor was not significant ($F = 1.98$, $P > 0.1$), although the interaction factor was significant ($F = 12.65$, $P = 0$).

The fact that the *actual* kinematics recorded in the FORCE condition showed a convergence trend toward the actual kinematics recorded in the BASELINE suggests the presence of an unaltered kinematic plan [see DISCUSSION in Shadmehr and Mussa-Ivaldi (1994)]. In other words, in the presence of the perturbing force, the monkeys gradually learned to transform the same *desired* kinematics into a new adapted dynamics (i.e., they acquired a new internal model for the dynamics). Note, incidentally, that the monkeys were not required to reach the peripheral target with a straight path and a bell-shaped speed profile. The fact that this convergence was not always completed within the span of trials and sessions that the monkeys engaged in the task does not alter this point because kinematic parameters were not found to plateau in the FORCE condition at values different from those recorded in the BASELINE. In other words, the kinematics continued to converge for as long as we kept the monkeys at work.

In conclusion, behavioral results offered in principle an interpretative framework whereby neuronal activity that did not change across conditions could be associated with the (desired) kinematics and neuronal activity that changed across conditions could be associated with the dynamics (see also DISCUSSION). The association between activity changes and movement dynamics was further supported by the comparison of changes observed for the activity of neurons and changes observed for electromyographic activity of muscles following adaptation (see following text).

In the analysis of EMG and neuronal activity, we disregarded in each condition the first 4 successful trials in each movement direction. Thus we essentially compared the activity recorded during the LATE BASELINE, LATE FORCE, and LATE WASHOUT subconditions, corresponding to the 3 *bottom panels* of Fig. 1*A*. For the sake of brevity, we refer in the following to these 3 subconditions as BASELINE, FORCE, and WASHOUT conditions. However, the analysis never included the "EARLY" part, unless otherwise specified.

EMG activity

The choice of viscous, curl force fields $\mathbf{F} = \mathbf{BV}$ offered two advantages. First, no perturbing force was ever present when the monkey held their hand still ($\mathbf{V} = 0$). In particular, no external force was ever present—even in the FORCE condition—during the instructed delay (DT). Second, the curl force field imposed predictable and consistent changes onto the EMG activity of muscles during the movement time (MT). Specifically, by comparing the preferred direction (Pd) recorded in the FORCE condition with that recorded in the BASELINE, we observed a shift of Pd in the direction of the external force field.

Figure 4 illustrates the EMG activity of one representative muscle (triceps longhead). The 3 columns represent the 3 conditions (BASELINE, FORCE, and WASHOUT), and the 4 rows represent the 4 time windows (CH, DT, MT, and TH). In each panel, the muscle's tuning curve is plotted in blue in polar coordinates, and the preferred direction (Pd) is plotted in red. The Pd is defined only for directionally tuned EMG activity. It can be noticed that there is no directional activity in either the CH or the DT. With respect to the MT, the Pd of the muscle is oriented toward 21° in the BASELINE. In the FORCE condition—after adaptation to the CCK field—the Pd of the muscle shifts by 28° in the direction of the external force (the CCK direction). In the WASHOUT, the Pd of the muscle shifts back, essentially to that originally recorded in the BASELINE.

FIG. 2. Psychophysics motor adaptation and motor learning: perpendicular displacement and correlation coefficient. *A*: perpendicular displacement, one session. Figure shows for each trial (*x*-axis, trial number) the values of the perpendicular displacement of the actual hand trajectory from the straight line passing through the initial location and the peripheral target computed at peak speed; the *y*-axis represents a normalized measure of distance, whereby the distance between the center location and the peripheral target equals 1. Each dot represents one trial, and positive values indicate a displacement in the direction of the external force. Displacement remains essentially constant and close to zero throughout the BASELINE (black color). In the CK FORCE (blue color) the displacement is initially greater than zero, and gradually return to values similar to that observed in the BASELINE as the monkey adapts. A clear aftereffect can be observed in the WASHOUT (green color), before the monkey readapts to the nonperturbed conditions. Solid lines are the result of linear fits. *B*: correlation coefficient, one session. For each trial, the correlation coefficient (CC) quantifies the similarity between actual speed profile and an ideal speed profile. The CC (*y*-axis) is plotted here against the trial number (*x*-axis). The CC ranges in values between −1 and 1, and is close to 1 when the speed profile is close to ideal. In the BASELINE, the CC has high values (CC about 0.98). When we introduce the CK FORCE, the CC drops sharply (CC <0.80). As the monkey adapts, the CC gradually recovers. When the force is then removed, we observe the aftereffect (CC about 0.93), before the monkey fully readapts. A statistical analysis indicated a significant difference between the CC recorded in the first 50 successful trials in the WASHOUT and the CC recorded in the last 50 successful trials in the BASELINE ($P < 0.002$, ANOVA). The values of the CC are smoothed in 10-trial bins. *C*: perpendicular displacement, all sessions. For each session, we computed the mean perpendicular displacement separately in the 3 conditions BASELINE (black triangles), FORCE (blue circles), and WASHOUT (green inverted triangles). The results are shown here for all the sessions and for the 2 monkeys. A clear effect of long-term learning can be observed because the mean perpendicular displacement in the FORCE gradually converged to the values observed in the BASELINE. *D*: correlation coefficient, all sessions. For each session, we averaged the CC over trials, separately in the 3 behavioral conditions (BASELINE, FORCE condition, WASHOUT). Two panels show the data for all the sessions and for the 2 monkeys. In each panel, the mean CC (*y*-axis) is plotted against the session number (*x*-axis), separately for the BASELINE (black triangles), the FORCE condition (blue circles), and the WASHOUT (green inverted triangles). For the BASELINE and the WASHOUT, the mean CC remained high throughout the recordings. For the FORCE condition, the mean CC increased over sessions (long-term learning). Note that the monkeys were still "learning" throughout the recording period.

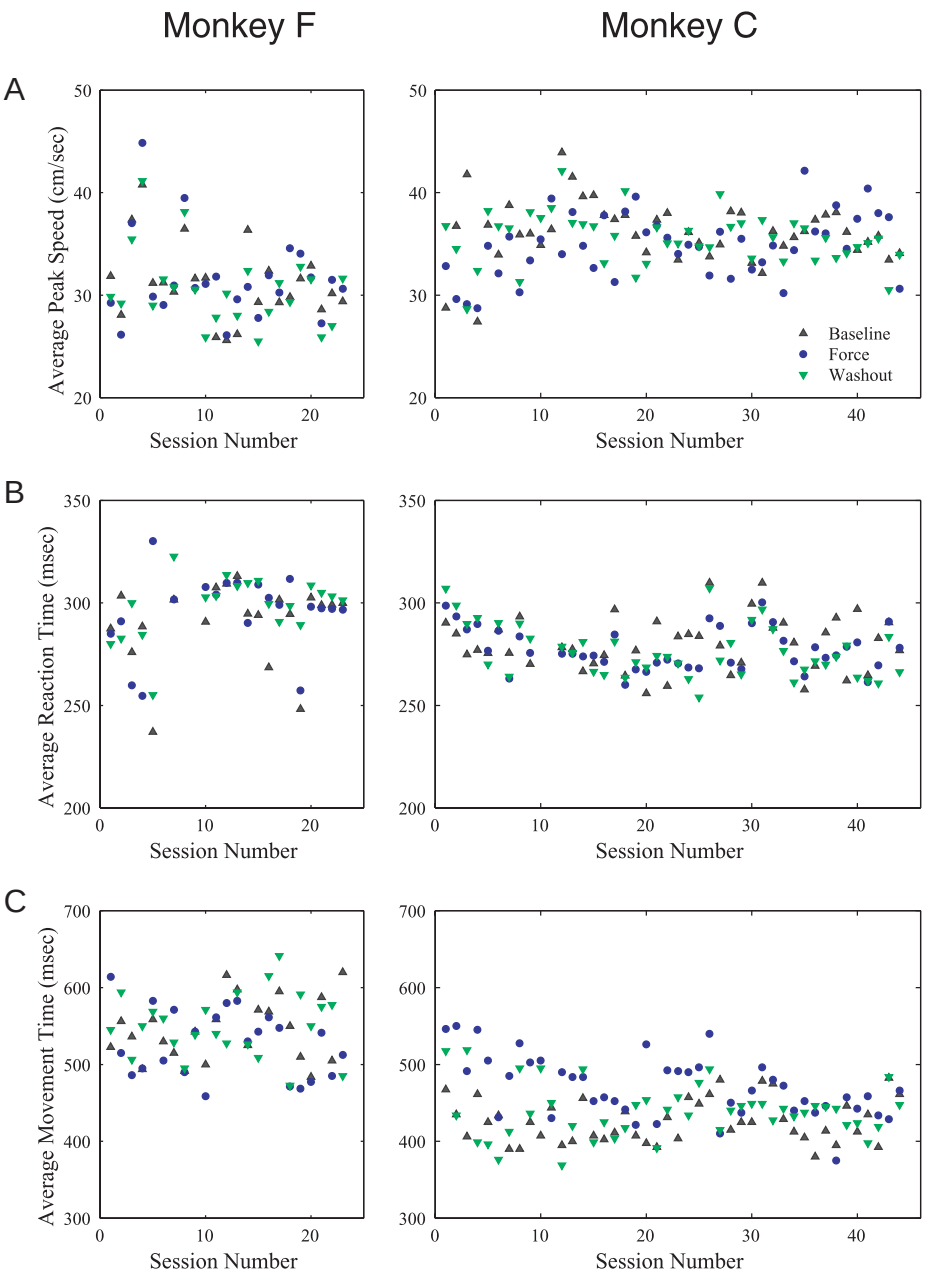

FIG. 3. Psychophysics: other kinematic parameters. Figure shows for each of the sessions in which neurons were actually recorded (*A*) the average peak speed, (*B*) the average reaction time, and (*C*) the average movement time [from movement onset (*mo*) to movement end (*me*)]. Color and symbol conventions are the same as in Fig. 2, *C* and *D*. CK and CCK FORCE sessions are combined for monkey C (*right panels*).

Similar shifts of Pd in the direction of the external force in the FORCE condition, and back in the opposite direction in the WASHOUT were observed for the population of muscles we recorded from. We defined the shift of Pd to be positive when it occurred in the direction of the external force, and we averaged across muscles. Considering the population of muscles, we found a significant shift of Pd in the FORCE condition compared with the BASELINE (mean shift = 19.2°; $P < 0.003$, 2-tailed circular *t*-test (Fisher 1993, p. 76)), a significant shift back in the WASHOUT compared with the FORCE condition (mean shift = −15.4°; $P < 0.03$, circular *t*-test), and no significant shift when the WASHOUT was compared with the BASELINE (mean shift = 4.4°; $P = 0.06$, circular *t*-test). Muscles were also classified with the same criteria used for cells, as shown in Table 1.

The shift of Pd observed for muscles is simply predicted considering the mechanics of the forces acting on the hand of the monkey in the FORCE condition, and has been described for both humans (Shadmehr and Moussavi 2000; Thoroughman and Shadmehr 1999) and monkeys (Li et al. 2001). For the current purposes, the crucial point is that the Pd of all the muscles shifts in the *same* direction (the direction of the external force field), independently of the initial Pd. Thus the shift of Pd observed for muscles provided a framework to interpret the neuronal data.

Neuronal database

We recorded the activity of 252 SMA cells in the adaptation task. In addition, we recorded the activity of 46 SMA cells in control sessions. Recordings were concentrated in the arm region of SMA (Fig. 5).

Figure 6 shows the distribution of preferred directions for the entire SMA population in the 3 behavioral conditions, and

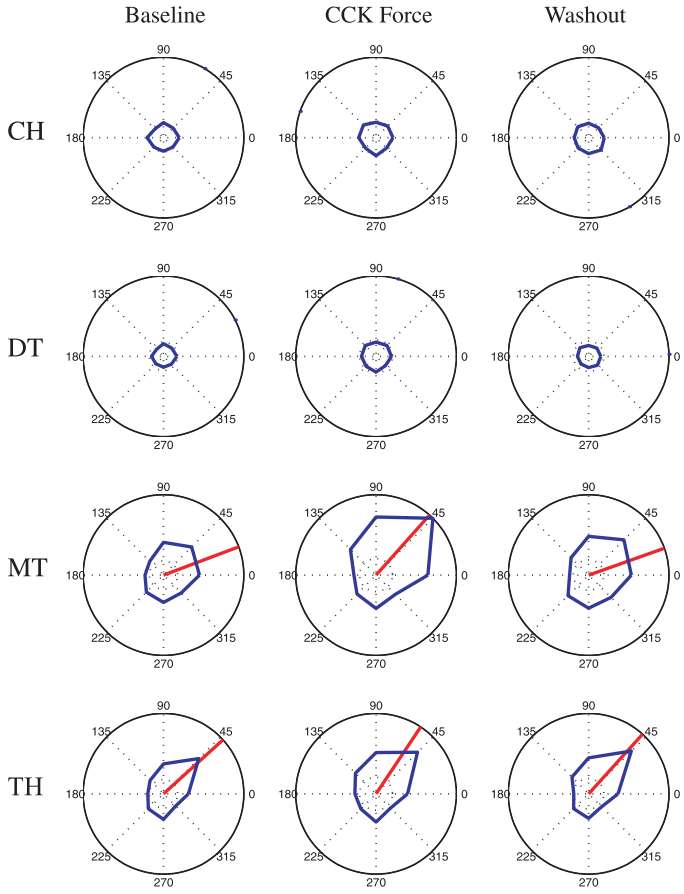

FIG. 4. Electromyographic (EMG) activity of the triceps-longhead muscle, recorded with the CCK force field. The tuning curve (blue) and the Pd (red) are plotted in polar coordinates, separately for the 4 time windows (CH, DT, MT, TH) and for the 3 conditions (BASELINE, FORCE condition, WASHOUT). The activity is normalized to the maximum across the 12 panels, and the Pd is defined only for directionally tuned activity. No directional EMG are present in either the CH (*1st row*) or the DT (*2nd row*). Considering the MT (*3rd row*) in the FORCE condition, the EMG activity modifies compared with the BASELINE, and the Pd shifts in the CCK direction (i.e., the direction of the external force). Shift of Pd in direction of the external force was consistent for all muscles and attributed to the vector sum between the force of the muscle and the external force. In the WASHOUT, the activity of the muscle returned to that observed in the BASELINE, and the Pd shifted back. With respect to the TH (*4th row*), we observed a more modest shift, which was not consistent for all the muscles. This suggests that the EMG activity in the TH was positional because viscous force fields ($\mathbf{F} = \mathbf{BV}$) equal zero when the hand is still ($\mathbf{V} = 0$).

Figs. 7–13 illustrate the activity of 6 representative cells recorded in SMA in the adaptation task (Figs. 7–12) and one control cell (Fig. 13). For each cell, we show the activity recorded in the 3 behavioral conditions (columns BASELINE, FORCE, and WASHOUT), and in the 4 time windows (rows CH, DT, MT, and TH), plotted in polar coordinates. For clarity of exposure, we describe different aspects observed in the activity of single neurons in separate sections here below.

Directional tuning

The percentages of directionally tuned cells for the 3 behavioral conditions and in the 4 time windows are shown in Table 2. In total, 44–49% of cells (depending on the behavioral condition) were directionally tuned in the delay time (DT). These percentages increased in the movement time (MT), to 59–66%. In the target hold time (TH), 53–58% of cells were tuned.

We also analyzed the circular distribution of Pd for the entire population (Fig. 6*A*). The null hypothesis of homogeneity held for all 3 conditions, and all 3 time windows (minimal $P > 0.04$, Rayleigh test), with the only exception of the FORCE condition and MT time window ($P < 0.002$, Rayleigh test). Consistent with previous studies (Crutcher and Alexander 1990), we found a broad correspondence when comparing the Pd recorded in different time windows (Fig. 6*B*).

Field-specific cells, tune-in cells, and tune-out cells

As the monkey adapted to the perturbing force, the activity of neurons in SMA changed. Some cells that were not tuned in the BASELINE became tuned in the FORCE condition after the adaptation, and lost their tuning again in the WASHOUT. Other cells that were originally tuned in the BASELINE lost their tuning in the FORCE condition, to regain it in the WASHOUT. These 2 types of cells were grouped in the class of "field-specific" cells. The changes observed in their directional tuning appeared dynamic in nature. Figure 7 illustrates one example of field-specific cell (MT activity). In total, field-specific cells accounted for 10% of SMA population (MT time window).

Another group of cells—designated "tune-in" cells—were initially not tuned in the BASELINE and acquired a directional tuning in the FORCE condition (Gandolfo et al. 2000). Unlike field-specific cells, however, tune-in cells maintained their newly acquired tuning in the WASHOUT, after the monkey had readapted to the nonperturbed conditions. Thus tune-in cells appeared to maintain a trace of the adaptation experience after readaptation in the WASHOUT. One example of tune-in cell is illustrated in Fig. 8. We also found a group of cells—designated "tune-out" cells—that were initially tuned in the BASELINE, lost their tuning in the FORCE condition, and failed to regain their tuning in the WASHOUT. Thus the changes observed for tune-in cells and tune-out cells appeared memory in nature. In total, tune-in cells and tune-out cells counted for 14 and for 8% of the population, respectively (analysis done on the MT activity).

Changes of preferred direction: delay time

Only cells that remained directionally tuned throughout the 3 conditions were analyzed and classified for their changes in

TABLE 1. *Muscles, electromyographic activity (EMG)*

	Preferred Direction (Pd)		Average Firing Frequency (Avf)		Tuning Width (Tw)	
	MT	TH	MT	TH	MT	TH
Kinematic	4 (29)	8 (62)	3 (20)	2 (13)	3 (25)	5 (50)
Dynamic	6 (43)	2 (15)	3 (20)	5 (33)	6 (50)	2 (20)
Memory I	2 (14)	1 (8)	3 (20)	6 (40)	2 (17)	3 (30)
Memory II	1 (7)	1 (8)	2 (13)	1 (7)	1 (8)	0 (0)
Other (*x*-*y*-*z*)	1 (7)	1 (8)	4 (27)	1 (7)	0 (0)	0 (0)
N EMG (tot)	14	13	15	15	12	10

Values are percentages, n = number of muscles. Results of classification for EMG traces. Each table cell reports the number (percentage) of muscles in the corresponding class. The bottom raw (N EMG) reports the total number of muscles available for analysis relatively to the particular parameter and time window. Only MT and TH time windows appear in the table because there was no EMG activity in the DT.

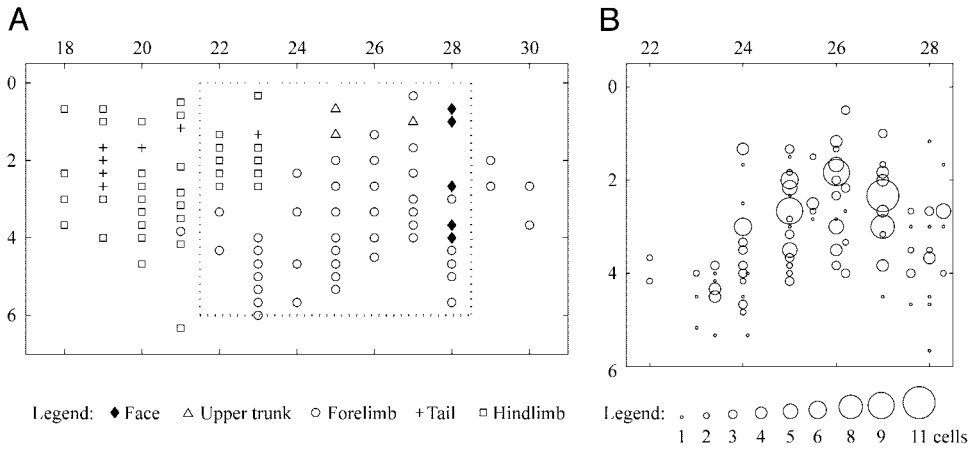

FIG. 5. Recording locations. *A*: microstimulation. Figure shows the results of microstimulation of the left medial wall of monkey C: *x*-axis indicates rostrocaudal position in stereotaxic coordinates; *y*-axis indicates depth of penetration (in mm). Somatotopic organization of SMA is clearly visible. *B*: recordings. Recordings were confined to the arm region of SMA (enlarged view here).

the preferred direction (Pd). Cells were classified separately for the DT, MT, and TH time windows.

Figure 9 illustrates the activity of a kinematic cell, classified according to the changes of Pd. Considering the DT time window (*2nd row*), the Pd of the cell remains essentially constant throughout the session (*x*-*x*-*x*). Because the desired kinematics remained unchanged throughout the 3 conditions, this cell was classified as a kinematic cell.

Figure 10 illustrates the activity of a dynamic cell recorded with a CK force field, and classified according to the changes of Pd. The DT activity is shown in the *2nd row*. In the FORCE condition, the Pd of the cell shifts in the direction of the

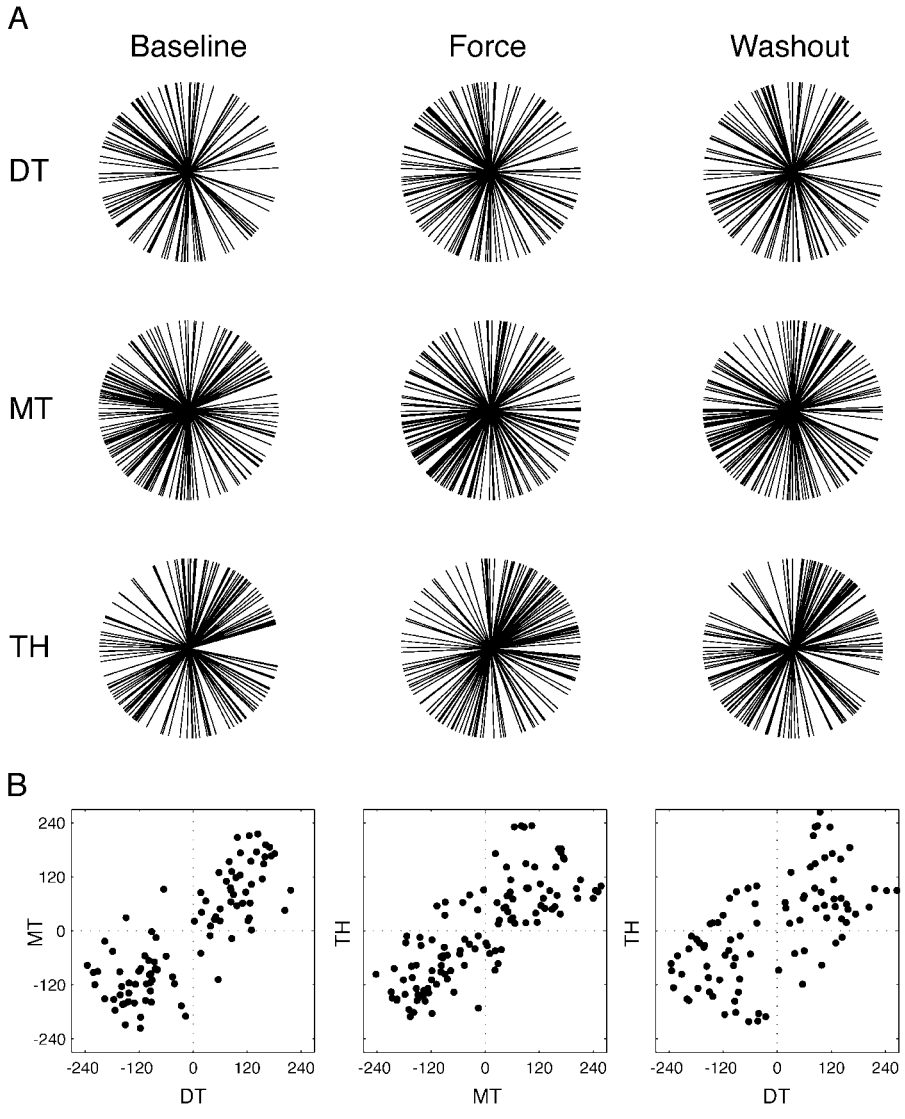

FIG. 6. Preferred directions (Pd). *A*: distribution of Pd. All SMA neurons are shown. Circular statistics indicated that the distribution of Pd around the clock was always homogeneous (minimal $P > 0.04$, Rayleigh test), except for the FORCE condition-MT time window ($P < 0.002$, Rayleigh test). *B*: comparing the Pd across time windows. *Left panel*: plot of the Pd recorded in the DT time window (*x*-axis) against the Pd recorded in the MT time window (*y*-axis). Each dot represents one cell. Note the broad correspondence between the Pd in the 2 time windows; the other 2 panels show the contrast between the Pd in the MT and that in the TH (*center panel*), and between the Pd in the DT and that in the TH (*right panel*).

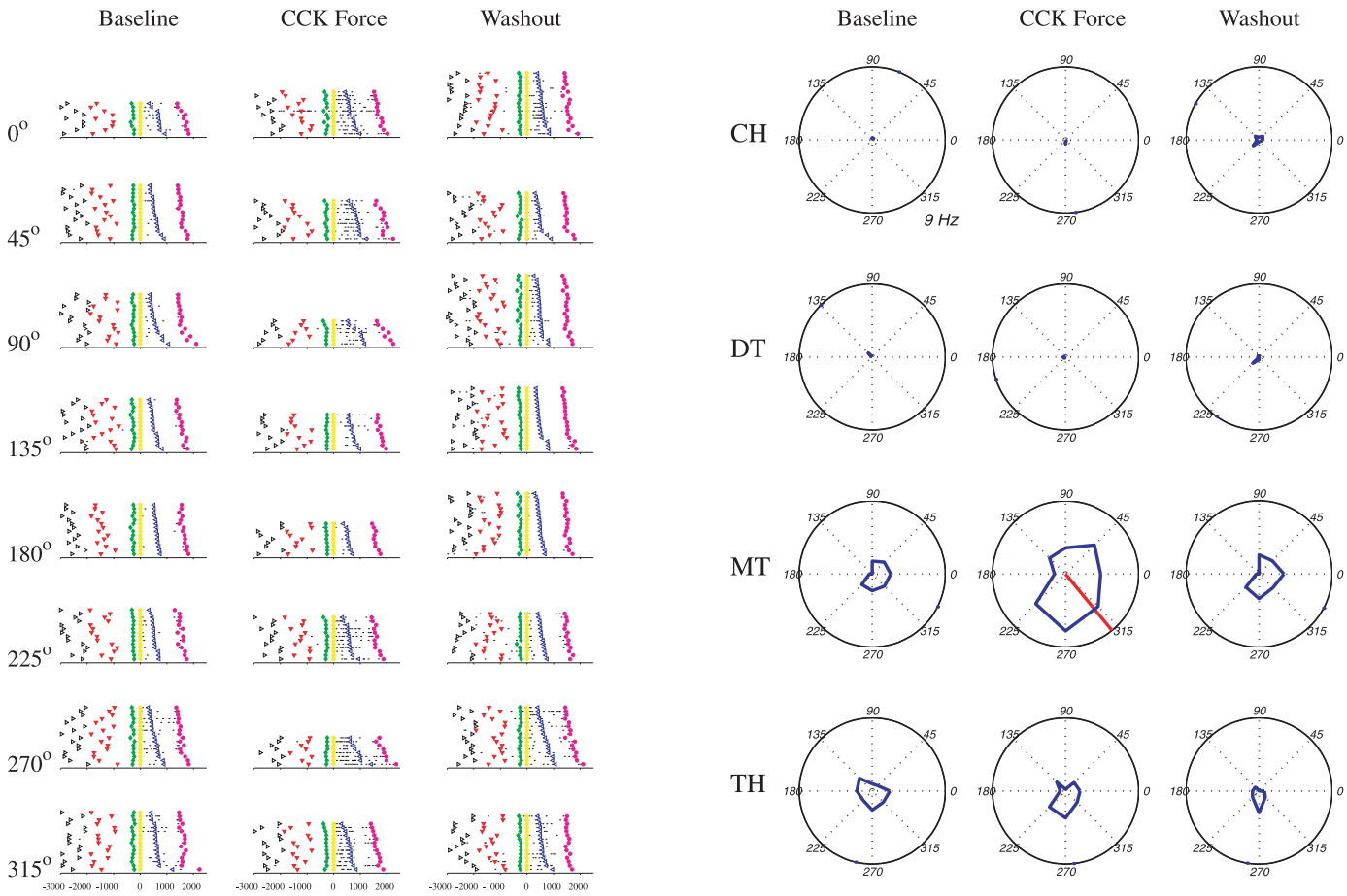

FIG. 7. A field-specific cell. *Left*: raster plots obtained for the 3 conditions (columns), separately for each of the 8 movement directions. Each line represents one trial and each small black dot represents one spike. Trials are aligned at the *mo* (yellow circle) and ranked according to the duration of the movement. For each trial, the raster illustrates the activity from the beginning of the trial to the end of the trial. Other symbols indicate the beginning of trial (black right triangle), the presentation of the *cue* (red inverted triangle), the *go* signal (green diamond), the *me* (blue left triangle), and the reward (*rew*, magenta circle). All the trials with reaction time (RT) such that (200 ms) $<$ RT $<$ (400 ms) are shown. *Right*: tuning curve of the cell is plotted in blue in polar coordinates, separately for the 3 conditions and for the 4 time windows. Pd—defined only for directionally tuned activity—is plotted in red. Radial scale (9 Hz) is the same for all 12 panels, and is indicated in *italics* for the *top left panel* (CH, BASELINE). Activity of this cell was very scarce in the CH and DT, throughout the 3 conditions. Considering the MT (*3rd row*), low activity and no directional tuning is present in the BASELINE. In the FORCE condition, the activity increases and the cell becomes directionally tuned. In the WASHOUT, however, the activity of the cell returns to that observed in the BASELINE and the cell loses its directional tuning. These changes are dynamic in nature, given that the dynamics of the movement were the same in the BASELINE and in the WASHOUT, but different in the FORCE condition.

external force (i.e., in the CK direction) compared with the BASELINE. In the WASHOUT, the Pd shifts in the opposite direction, back to that recorded in the BASELINE (*x-y-x*). Because the dynamics of the movement were the same in the BASELINE and in the WASHOUT, but different in the FORCE condition, this cell was classified as a dynamic cell.

TABLE 2. *SMA, cells directionally tuned*

	Condition		
Time Window	BASELINE	FORCE	WASHOUT
CH	32 (13%)	34 (13%)	17 (7%)
DT	110 (44%)	124 (49%)	117 (46%)
MT	149 (59%)	165 (65%)	166 (66%)
TH	136 (54%)	133 (53%)	145 (58%)

The table indicates—for each condition and time window—the number (percentage) of directionally tuned cells recorded in SMA with the force field adaptation task ("experimental cells"). CH, center hold; DT, delay time; MT, movement time; TH, target hold.

Figure 11 illustrates the activity of a memory I cell recorded in SMA with a CCK force field, and classified according to the changes of Pd. Again, the DT activity is illustrated in the *2nd row*. In the FORCE condition, the Pd of the cell shifts in the direction of the external force (i.e., the CCK direction) compared with the BASELINE. However, after readaptation in the WASHOUT, the Pd remained oriented in the newly acquired direction (*x-y-y*). Thus the cell appeared to maintain a trace of the previously adaptation experience. We therefore classified this cell as a memory I cell.

Considering the entire SMA population, a total of 68 cells could be classified according to their changes of Pd in the DT time window. The majority of these cells was classified as kinematic (51 cells, 75%). However, we also found dynamic cells (3 cells, 4%), memory I cells (9 cells, 13%), and memory

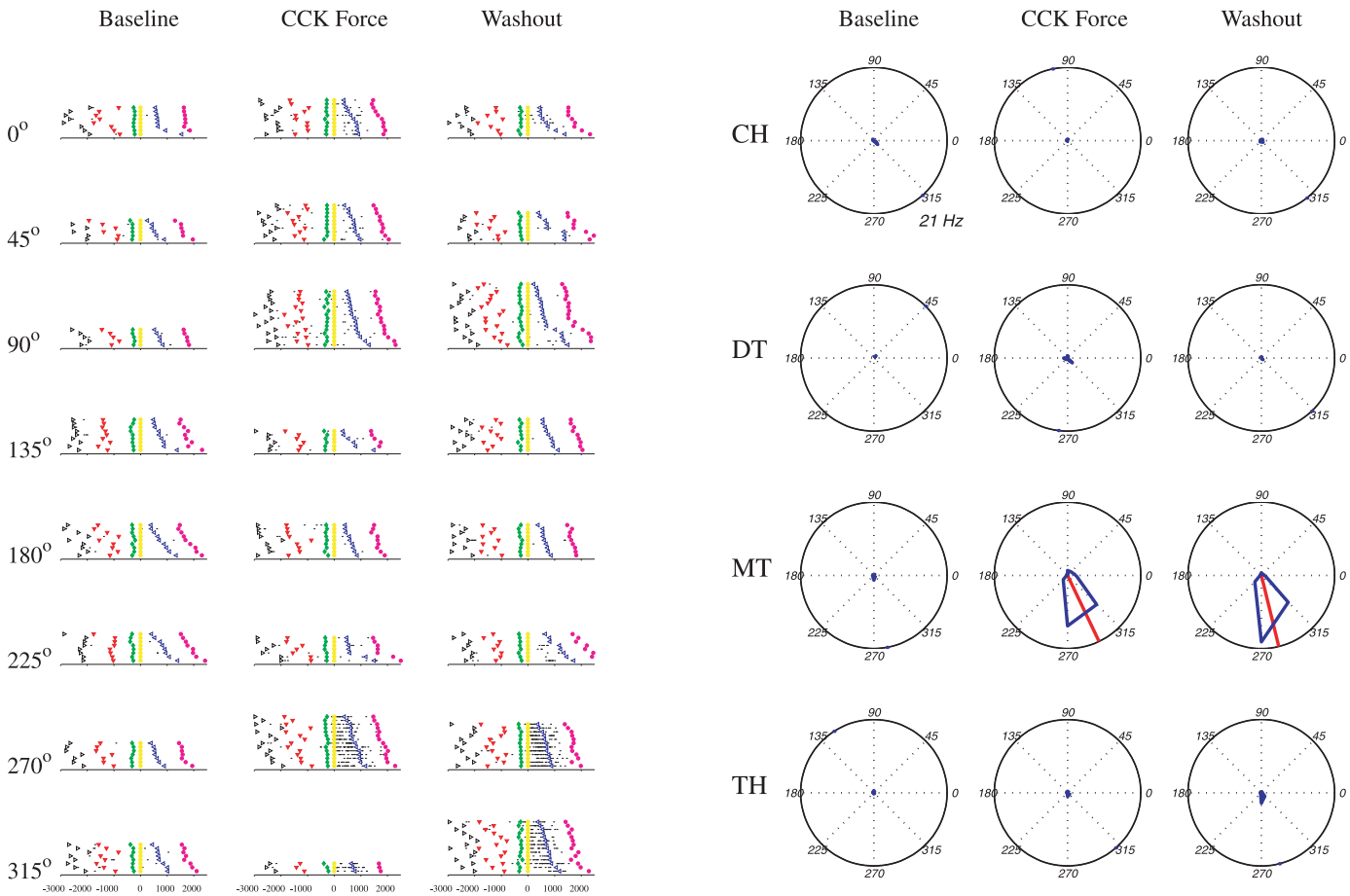

FIG. 8. A "tune-in" cell. *Left*: raster plots. All conventions are as in Fig. 7. *Right*: CH, DT, and TH activity of this cell remained scarce throughout the session. Considering the MT (*3rd row*), scarce activity is present in the BASELINE. However, after adaptation in the FORCE condition, the cell becomes sharply tuned. In the WASHOUT, after the monkey readapts to the nonperturbed conditions, the cell maintains the new directional tuning. Thus this cell maintains a memory of the newly acquired internal model for the dynamics. All conventions are as in Fig. 7.

II cells (5 cells, 7%). These percentages are summarized in Table 3*a*.

We also analyzed the shifts of Pd at the population level. We computed the shift of Pd for each cell, and defined positive the shifts that occurred in the direction of the external force. We then averaged the shift of Pd across the SMA population, for the 3 between-conditions comparisons (FORCE–BASELINE; WASHOUT–FORCE; WASHOUT–BASELINE). Comparing the FORCE with the BASELINE, we found that neurons in SMA shifted their Pd significantly in the direction of the external force (mean shift = 11.1°; $P < 0.02$, circular *t*-test). Conversely, SMA neurons shifted their Pd back in the opposite direction in the WASHOUT compared with the FORCE condition, though this shift did not reach significance (mean shift = −7.2°; $P = 0.054$, circular *t*-test). No significant shift of Pd was observed for the population when comparing the WASHOUT with the BASELINE (mean shift = 5.6°; $P = 0.3$, circular *t*-test). These changes of Pd observed for the neuronal population are summarized in Table 4*a*.

Qualitatively, the shifts of Pd observed for SMA neurons during the delay (DT) match the shifts of Pd observed for muscles during the upcoming movements (MT). Three points should be stressed, however. First, no EMG activity was present during the DT (see Fig. 4). Second, no force was actually present ($\mathbf{F} = \mathbf{BV} = 0$) because the monkey was not moving ($\mathbf{V} = 0$). Third, because the extent of the delay was randomly chosen, the monkey could not preinitiate the movement. It was also observed that the Pd of SMA cells shifted increasingly over the course of the delay, and that the extent of the shift in the DT time window correlated with the goodness of adaptation (quantified by the initial direction of the upcoming movement) and anti-correlated with the following reaction time (Padoa-Schioppa et al. 2002).

Changes of preferred direction: movement time

The classes of kinematic, dynamic, and memory I cells are illustrated for the DT time window in Figs. 9–11 (*2nd rows*). Similar classes of cells were also found for the MT time window, as illustrated in the same Figs. 9–11 (*3rd rows*). Considering the MT activity of the cell in Fig. 9 (*3rd row*), the Pd is essentially constant throughout the 3 conditions (*x*-*x*-*x*). Therefore the cell was classified as kinematic for the changes of Pd in the MT.

The cell in Fig. 10 was recorded with a CK force field. Considering the MT activity (*3rd row*), the Pd of the cell shifts in the direction of the external force in the FORCE condition compared with the BASELINE. In the WASHOUT, the Pd shifts back in the opposite direction, essentially to its original orientation

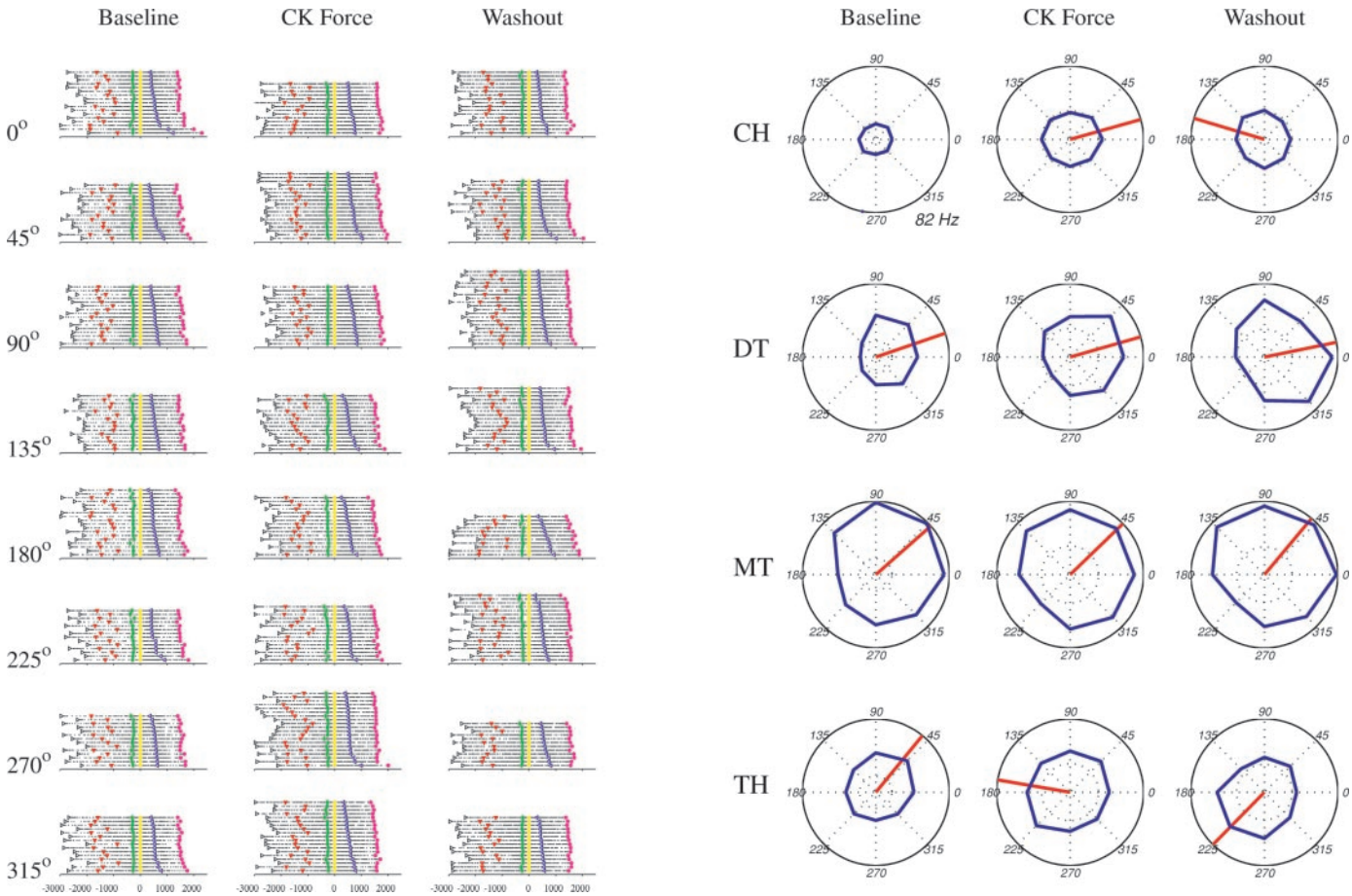

FIG. 9. A kinematic cell (*x-x-x*). Left: raster plots. All conventions are as in Fig. 7. *Right*: considering either the DT (*2nd row*) or the MT (*3rd row*), the Pd of the cell remains essentially constant throughout the 3 conditions. We classified this cell as kinematic for its changes of Pd because the desired kinematics of the movement remained the same throughout. Note that—unlike the Pd—the Avf of the cell changed across conditions. Considering for instance the changes of Avf in the CH, the cell has memory I properties. All conventions are as in Fig. 7.

(*x-y-x*). Therefore the cell was classified as dynamic for the changes of Pd in the MT.

The cell in Fig. 11 was recorded with a CCK force field. Again, considering the MT activity (*3rd row*), the Pd of the cell shifts in the direction of the external force in the FORCE condition compared with the BASELINE. In the WASHOUT, the cell maintains its newly acquired Pd (*x-y-y*). Thus this cell was classified as a memory I cell for the changes of Pd in the MT.

Figure 12 illustrates the activity of a memory II cell recorded in SMA with a CCK force field. In the DT (*2nd row*), the cell is not directionally tuned. Considering the MT time window (*3rd row*), the Pd is essentially unchanged in the FORCE condition compared with the BASELINE. In the WASHOUT, however, the Pd of the cell shifts in the direction *opposite* to the previously experienced force field, that is the CK direction (*x-x-y*). Thus this cell was classified as a memory II cell for the changes of Pd in the MT. Note that the shift of Pd of memory II cells seems to balance in the WASHOUT the shift of Pd of memory I cells (Li et al. 2001).

In total, we could classify 117 SMA cells according to their changes of Pd in the MT. Of these, 61 cells (52%) were kinematic, 20 cells (17%) were dynamic, 20 cells (17%) were memory I, 13 cells (11%) were memory II, and 3 cells (3%) were "other" cells. These percentages are summarized in Table 3*a*.

Considering the entire population of SMA in the MT, we observe shifts of Pd similar to that observed for the EMG activity of muscles, and for neurons in M1. As a population, neurons in SMA show a significant shift of Pd in the FORCE condition compared with the BASELINE (mean shift = 16.6°; $P < 10^{-6}$, circular *t*-test). Comparing the WASHOUT with the FORCE condition, we see a significant shift back in the opposite direction (mean shift = −9.7°; $P < 0.001$, circular *t*-test). In contrast, no significant shift is observed when comparing the WASHOUT and the BASELINE (mean shift = 3.9°; $P = 0.2$, circular *t*-test). The changes of Pd observed for the neuronal population are summarized in Table 4*a*.

Changes of preferred direction: target hold time

We found that some cells also changed their Pd in the TH. One case of memory I cell is shown in Fig. 11. The percentages of cells in the various classes are summarized in Table 3*a*. Considering the entire SMA population in the TH, however, we found no significant shifts of Pd in either the FORCE condition compared with the BASELINE (mean shift = 3.4°; $P = 0.3$, circular *t*-test) or in the WASHOUT compared with the FORCE condition (mean shift = −0.1°; $P = 1$, circular *t*-test). These averages are summarized in Table 4*a*.

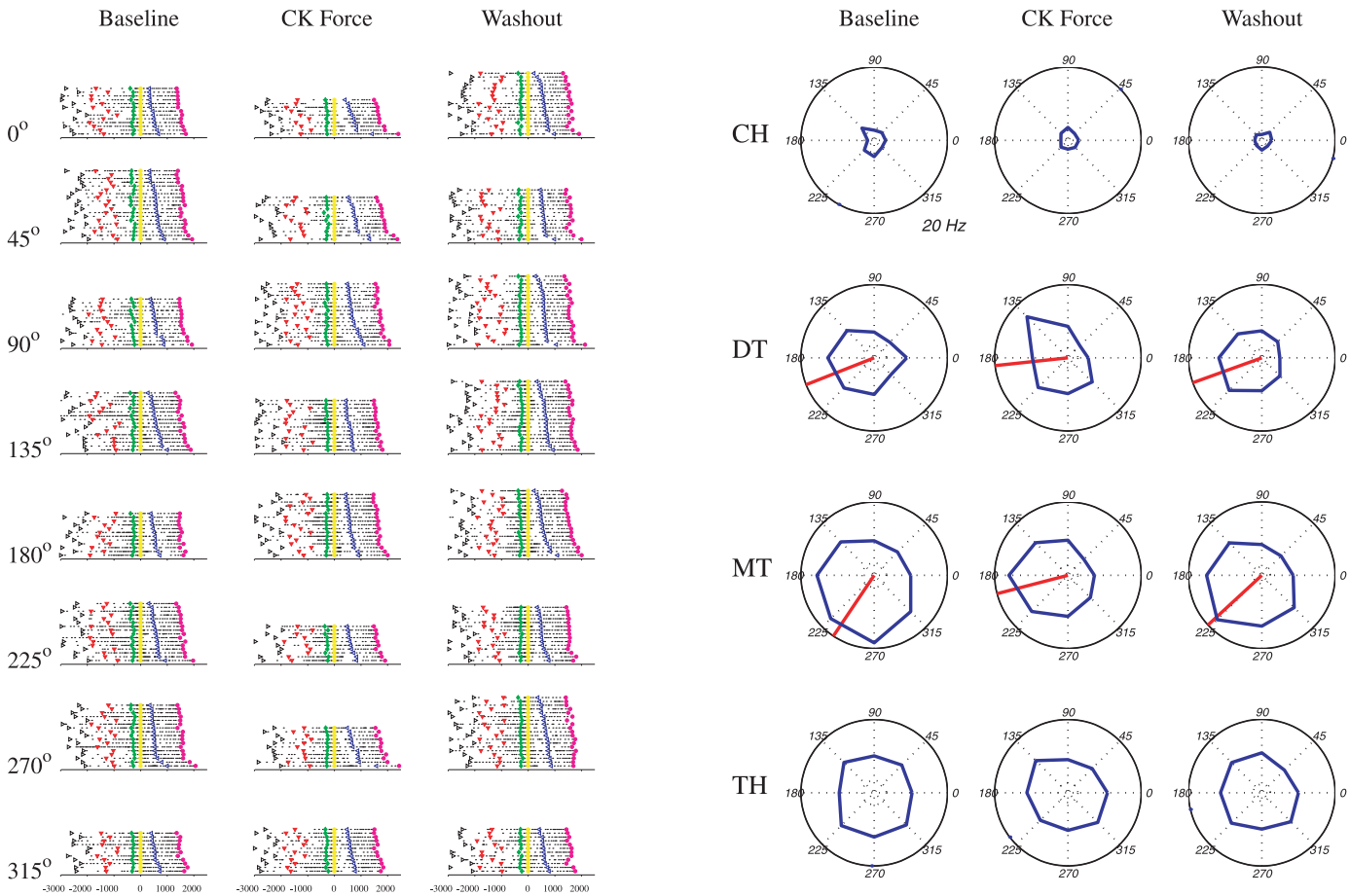

FIG. 10. A dynamic cell (*x-y-x*). *Left*: raster plots. All conventions are as in Fig. 7. *Right*: this cell was recorded with a CK force field. Cell is directionally tuned both in the DT and in the MT, in all 3 conditions. Considering the DT activity (*2nd row*), the Pd of the cell shifts in the FORCE condition compared with the BASELINE in the direction of the external force (CK direction). In the WASHOUT, the Pd of the cell shifts back to that observed in the BASELINE; thus we classified the cell as dynamic for its changes of Pd in the DT. Considering the MT activity (*3rd row*), the cell exhibits similar changes. Pd of the cell shifts in the CK direction in the FORCE condition, and shifts back in the WASHOUT essentially to that observed in the BASELINE; thus the cell was also classified as dynamic for its changes of Pd in the MT. Note that the shift of Pd is quantitatively more pronounced in the MT than in the DT, although qualitatively analogous in the 2 time windows. All conventions are as in Fig. 7.

Changes of average firing frequency

We analyzed the changes of average firing frequency (Avf) across behavioral conditions, and we classified all single SMA neurons separately in the CH, DT, MT, and TH time windows. Changes of Avf across conditions for individual neurons and at the population level were analyzed with the same criteria and procedures used for the changes of Pd, as described in METHODS.

The percentages of experimental cells classified as kinematic, dynamic, memory I, and memory II for their changes of Avf are reported in Table 3*a*. For example, the cell illustrated in Fig. 9 was classified as kinematic for its changes of Avf in the MT time window. The cell illustrated in Fig. 11 was classified as a memory I cell for its changes of Avf in both the MT and TH time windows.

At the level of individual cells, we observed both increases (e.g., Figs. 8 and 12) and decreases (e.g., Fig. 11) of Avf across conditions. Considering the entire population, we found a general increase in Avf in the FORCE condition compared with the BASELINE, and a further—although more limited—increase in Avf in the WASHOUT compared with the FORCE condition. The increase in Avf was present in all time windows, as summarized in Table 4*a*.

Changes of tuning width

We analyzed the changes of tuning width (Tw) of single cells across behavioral conditions, and we classified single SMA neurons separately in the DT, MT, and TH time windows. Changes of Tw across conditions for individual neurons and at the population level were analyzed with the same criteria and procedures used for the changes of Pd, as described in METHODS. The percentages of experimental cells classified as kinematic, dynamic, memory I, and memory II for their changes of Tw are reported in Table 3*a*.

Considering the entire population, we found a general increase in Tw in all time windows, both in the FORCE condition and in the WASHOUT. This increase, however, did not reach significance level, except for the MT time window, when the WASHOUT was compared with the BASELINE. The changes of Tw for the entire population are summarized in Table 4*a*.

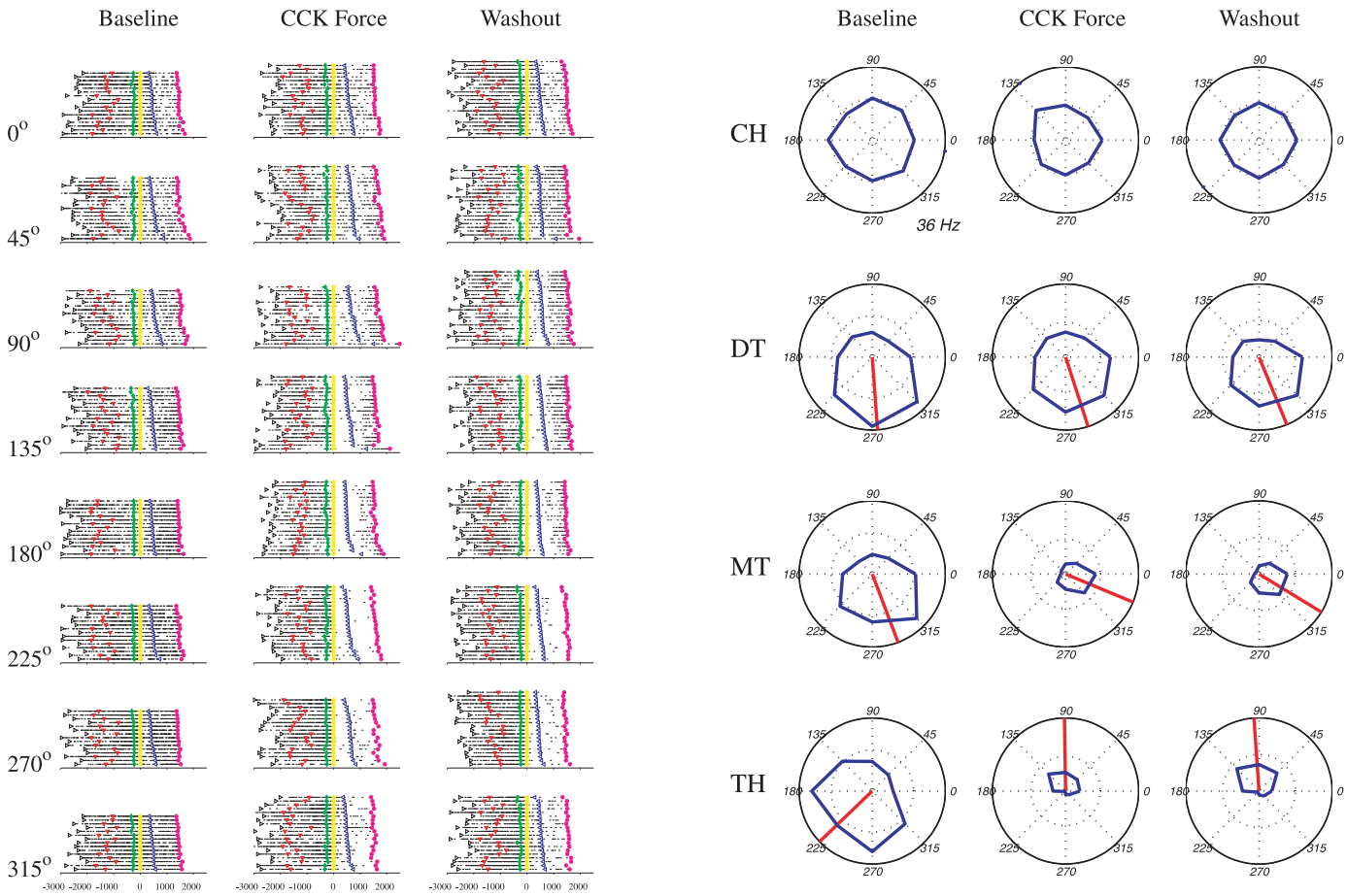

FIG. 11. A memory I cell (*x-y-y*). *Left*: raster plots. All conventions are as in Fig. 7. *Right*: activity of this cell—recorded with a CCK force field—is directionally tuned in the DT, MT, and TH time windows. Cell is classified as memory I cell for its changes of Pd in all 3 time windows. Considering—for instance—the DT activity (*2nd row*), the activity of the cell modifies in the FORCE condition compared with the BASELINE and the Pd shifts in the CCK direction (the direction of the external force). In the WASHOUT, the activity of the cell and the Pd remain as observed in the FORCE condition. Because the cell appeared to maintain a trace of the adaptation experience, we classified it as a memory I cell. Considering the MT time window, we observe similar changes. Here again, the shift of Pd (and the overall changes) are quantitatively more pronounced in the MT than in the DT, but qualitatively analogous. This cell was also classified as a memory I cell for its changes of average firing rate (Avf), in both the MT and TH time windows. In contrast, the CH activity of the cell remained stable throughout the session. All conventions are as in Fig. 7.

Control cells

Figure 13 illustrates the activity of one control cell, recorded in a session where no force field was ever introduced. Considering in particular the preferred direction (Pd), it can be seen that the Pd of the cell is relatively stable throughout the session, in all time windows. We analyzed all control cells ($n = 46$) with the same procedure used for experimental cells. Considering the entire population of control cells, no significant shifts of Pd were observed either in the FORCE condition or in the WASHOUT, in any time window (DT, MT, or TH; 9 comparisons total, maximal mean shift = 6.2°; minimal $P = 0.2$ circular *t*-test).

Considering individual cells, changes of Pd sometimes reached significance. Thus we classified the population of control cells with the same criteria used for experimental cells. In particular for the DT time window, the classification indicated that 18 of 20 control cells (90%) were kinematic. The remaining 2 cells were classified as memory I (5%) and memory II (5%). With respect to the MT time window, we found that 24 of 33 control cells (73%) were kinematic for their changes of Pd. Of the remaining, 4 cells (12%) were memory I and 5 cells (15%) were memory II. Similar results were found for the TH time window. We found that 20 of 21 control cells (95%) were kinematic, and the remaining one cell (5%) was dynamic.

To contrast this classification with that of experimental cells, we collapsed cells of each group into the kinematic and nonkinematic superclasses (nonkinematic cells included dynamics, memory I, memory II, and other cells). We then submitted the emerging 2 × 2 contingency table to the χ^2 analysis. In particular for the DT time window, although nonkinematic cells were more frequent among experimental cells than among controls, that difference did not reach significance level ($\chi^2 = 2.05$; $df = 1$; $P = 0.15$). For the MT time window, the χ^2 analysis indicated a significant difference between the control group and the experimental group of cells ($\chi^2 = 4.44$; $df = 1$; $P < 0.05$). In other words, there were comparatively more nonkinematic cells in the experimental group than in the control group. For the TH time window, the χ^2 analysis indicated a significant difference between control cells and experimental cells ($\chi^2 = 6.81$; $df = 1$; $P < 0.01$). In addition, inspection of

TABLE 3. *SMA, classification of cells in force-field adaptation task and in control sessions*

	Preferred Direction (Pd)			Average Firing Frequency (Avf)			Tuning Width (Tw)		
	DT	MT	TH	DT	MT	TH	DT	MT	TH
				a. SMA, experimental cells					
Kinematic	51 (75)	61 (52)	63 (67)	65 (32)	53 (23)	39 (19)	11 (65)	19 (59)	15 (52)
Dynamic	3 (4)	20 (17)	8 (9)	16 (8)	22 (10)	19 (9)	0 (0)	5 (16)	2 (7)
Memory I	9 (13)	20 (17)	14 (15)	53 (26)	61 (27)	66 (31)	2 (12)	4 (13)	7 (24)
Memory II	5 (7)	13 (11)	7 (7)	44 (21)	47 (21)	40 (19)	4 (24)	4 (13)	5 (17)
Other (*x*-*y*-*z*)	0 (0)	3 (3)	2 (2)	27 (13)	45 (20)	46 (22)	0 (0)	0 (0)	0 (0)
N cells (tot)	68	117	94	205	228	210	17	32	29
				b. SMA, control cells					
Kinematic	18 (90)	24 (73)	20 (95)	13 (34)	10 (22)	11 (29)	9 (100)	9 (69)	7 (64)
Dynamic	0 (0)	0 (0)	1 (5)	3 (8)	5 (11)	3 (8)	0 (0)	0 (0)	0 (0)
Memory I	1 (5)	4 (12)	0 (0)	9 (24)	12 (26)	7 (18)	0 (0)	3 (23)	1 (9)
Memory II	1 (5)	5 (15)	0 (0)	5 (13)	11 (24)	7 (18)	0 (0)	0 (0)	2 (18)
Other (*x*-*y*-*z*)	0 (0)	0 (0)	0 (0)	8 (21)	8 (17)	10 (26)	0 (0)	1 (8)	1 (9)
N cells (tot)	20	33	21	38	46	38	9	13	11

Results for SMA neurons recorded in the force field-adaptation task (*a*) and in control sessions (*b*). Each table cell reports the number (percentage) of neurons in the corresponding class. The bottom raw (N cells) reports the total number of cells available for analysis relatively to the particular parameter and time window.

TABLE 4. *SMA, population changes in force-field adaptation task and in control sessions*

	Between-Conditions Comparison		
	FORCE–BASELINE	WASHOUT–FORCE	WASHOUT–BASELINE
	a. SMA, experimental cells		
Change of Pd			
DT	m = 11.1° (*)	m = −7.2°	m = 5.6°
MT	m = 16.6° (**)	m = −9.7° (**)	m = 3.9°
TH	m = 3.4°	m = −0.1°	m = 4.3°
Change of Avf			
CH	m = 26% (**)	m = 12% (**)	m = 42% (**)
DT	m = 29% (**)	m = 14% (**)	m = 48% (**)
MT	m = 26% (**)	m = 1%	m = 21% (**)
TH	m = 30% (**)	m = 9% (*)	m = 36% (**)
Change of Tw			
DT	m = 8°	m = 10°	m = 23°
MT	m = 11°	m = −6°	m = 24° (*)
TH	m = 20°	m = −7°	m = 11°
	b. SMA, control cells		
Change of Pd			
DT	m = −3.4°	m = −4.5°	m = −4.9°
MT	m = 0.9°	m = −4.1°	m = 1.4°
TH	m = 0.6°	m = 6.2°	m = 4.0°
Change of Avf			
CH	m = 23% (*)	m = 12%	m = 36% (*)
DT	m = 35%	m = 8%	m = 50% (*)
MT	m = 14% (*)	m = 5%	m = 19% (*)
TH	m = 20%	m = 9%	m = 34%
Change of Tw			
DT	m = 23°	m = −17°	m = 9°
MT	m = −11°	m = 7°	m = 3°
TH	m = −9°	m = 15°	m = 13°

For each comparison and each time window, "m" indicates the average change. Asterisks indicate changes at the significance levels of $P < 0.05$ (*) and $P < 0.001$ (**), as indicated by circular (Pd and Tw) and linear (Avf) *t*-tests. Pd, preferred direction; Avf, average firing frequency; Tw, tuning width.

single-matrix elements revealed that nonkinematic cells were significantly less frequent in the control group (decomposed $\chi^2 = 4.01$; $df = 1$; $P < 0.05$) than would be expected by chance.

With respect to changes of Avf, it can be observed in Fig. 13 that the activity of the control cell increased across behavioral conditions. This increase was generally consistent for the population of control cells and for all time windows.

Analysis on the Tw revealed no significant changes for the population of control cells. Likewise, individual control cells rarely presented significant changes of Tw.

The results of the classification of control cells for each parameter and time window are summarized in Table 3*b*. Changes for the population of control cells are summarized in Table 4*b*.

Summary of activity changes: comparing experimental cells and control cells

Figure 14 illustrates the changes observed at the level of the population for all the 4 time windows considered (CH, DT, MT, and TH) and for the 3 parameters, preferred direction (Pd), average firing frequency (Avf), and tuning width (Tw). Experimental cells (*left*) and control cells (*right*) are considered separately. With respect to the changes of Pd, experimental cells present a significant shift in the FORCE condition and back in the WASHOUT, in both the DT and MT time windows. In contrast, no such shift is observed in control cells. With respect to the Avf, both experimental and control cells show an increase of activity across conditions, in all time windows, although this effect is more pronounced for experimental cells. With respect to the Tw, experimental cells show an increase across conditions in both the DT and MT time windows, which reaches significance level in the WASHOUT for the MT time window. In contrast, the Tw of control cells appears essentially stable throughout conditions. These results are also summarized in Table 4*b*.

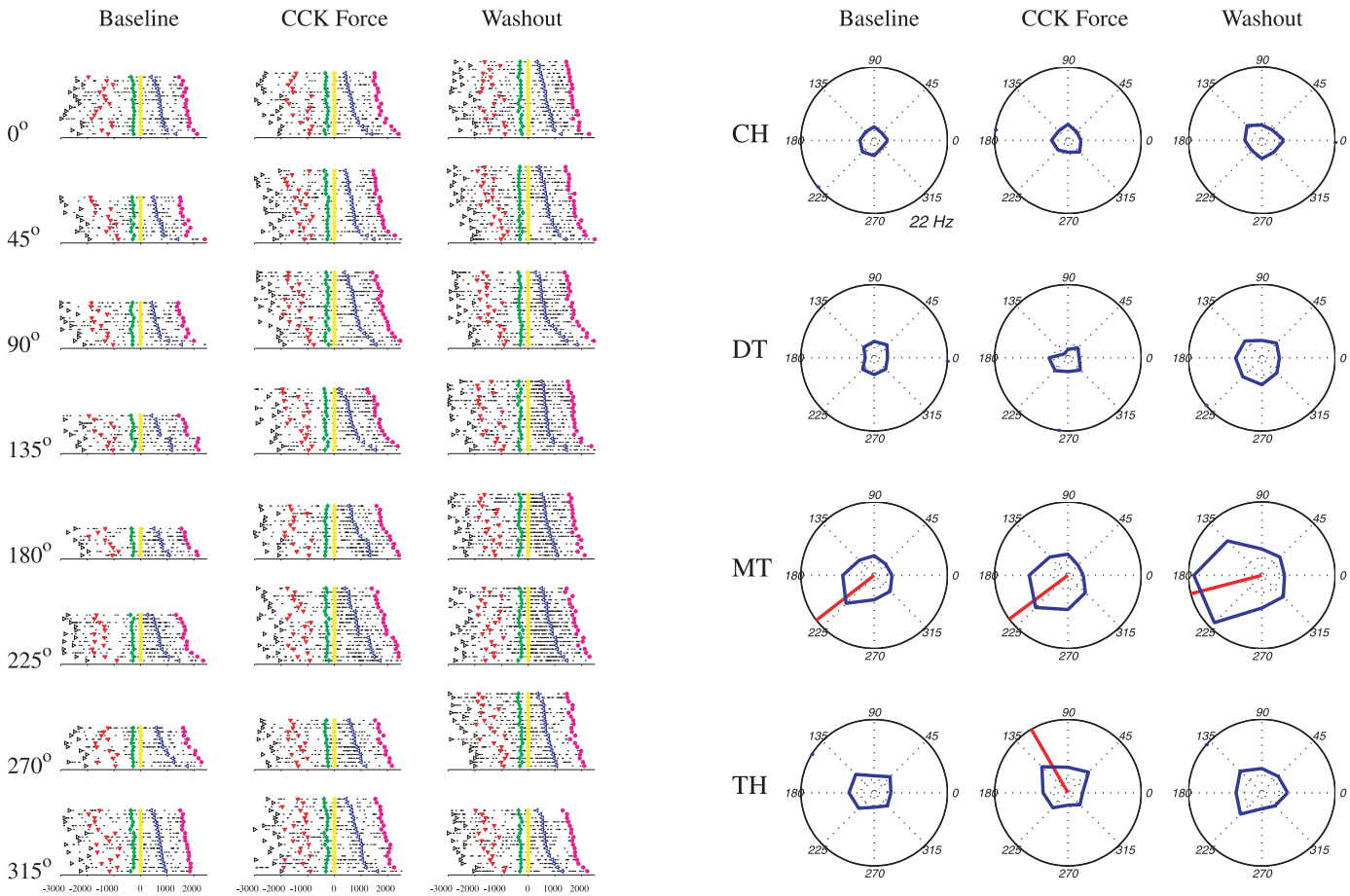

FIG. 12. A memory II cell (*x*-*x*-*y*). *Left*: raster plots. All conventions are as in Fig. 7. *Right*: activity of this cell—recorded with a CCK force field—is directionally tuned in the MT throughout the 3 conditions. In the FORCE condition, the activity of the cell remained essentially unchanged compared with the BASELINE. In the WASHOUT, however, the activity modified, and the Pd shifted in the CK direction, that is the direction *opposite* to the previously experienced external force; thus the cell was classified as a memory II cell. All conventions are as in Fig. 7.

Figure 15 illustrates the classification of cells with respect to the changes of preferred direction (Pd) in the DT, MT, and TH time windows, separately for experimental cells (*left*) and control cells (*right*). In each scatter plot, the *x*-axis represents the shift of Pd in the FORCE compared with BASELINE; the *y*-axis represents the shift of Pd in the WASHOUT compared with the FORCE. Positive values indicate shifts of Pd in the direction of the external force, and each data point represents one neuron. Neurons are color-coded according to their class, and the pie on the *upper right* of each plot summarizes the percentages of cells in each class. Kinematic cells (empty symbols), which do not shift Pd in either the FORCE or the WASHOUT, lie close to the origin. Dynamic cells (blue color), which present significant and opposite shift in the 2 measures, lie on the diagonal crossing the 2nd and 4th quadrants. Memory I cells (green color) and memory II cells (red color), which shift Pd in only one of the 2 measures, lie close to the *x*-axis and *y*-axis, respectively.

Figure 16 illustrates the classification of cells with respect to the changes of Tw for experimental cells and control cells, in a format similar to that of Fig. 15. It can be noticed that the incidence of nonkinematic cells is higher for experimental cells, in all 3 time windows.

Consistency of classification across time windows: DT and MT

The cells shown in Figs. 9–11 appear to have a rather consistent change of Pd across time windows. For instance, the cell in Fig. 10 is classified as dynamic for its changes of Pd recorded in either the DT or the MT. Were cells always as consistent? To address this question, we combined the classification in the DT with that in the MT in a 5 × 5 contingency table, which we analyzed with a χ^2 statistics. With respect to the changes of Pd, however, no cells were classified as "other" in the DT time window. Analysis of the remaining 4 × 4 contingency table did not provide evidence to reject the null hypothesis of homogeneity (Pearson's $\chi^2 = 8.07$, $df = 9$, $P = 0.5$). Further computing the trace $Tr = \Sigma_{i=j} \chi^2_{ij}$ we quantified whether the classification across time windows coincided more often than expected by chance. We found no statistical evidence of such consistency ($Tr = 1.63$, $df = 3$, $P = 0.8$). We repeated this analysis by collapsing cells in 3 superclasses of kinematic, dynamic, and memory cells (memory cells included memory I, II, and other cells) and we obtained a similar result (Pearson's $\chi^2 = 5.37$, $df = 4$, $P = 0.25$; $Tr = 2.3$, $df = 2$, $P = 0.7$).

With respect to the changes of Avf, in contrast, we found that the classification in the DT and MT time windows were

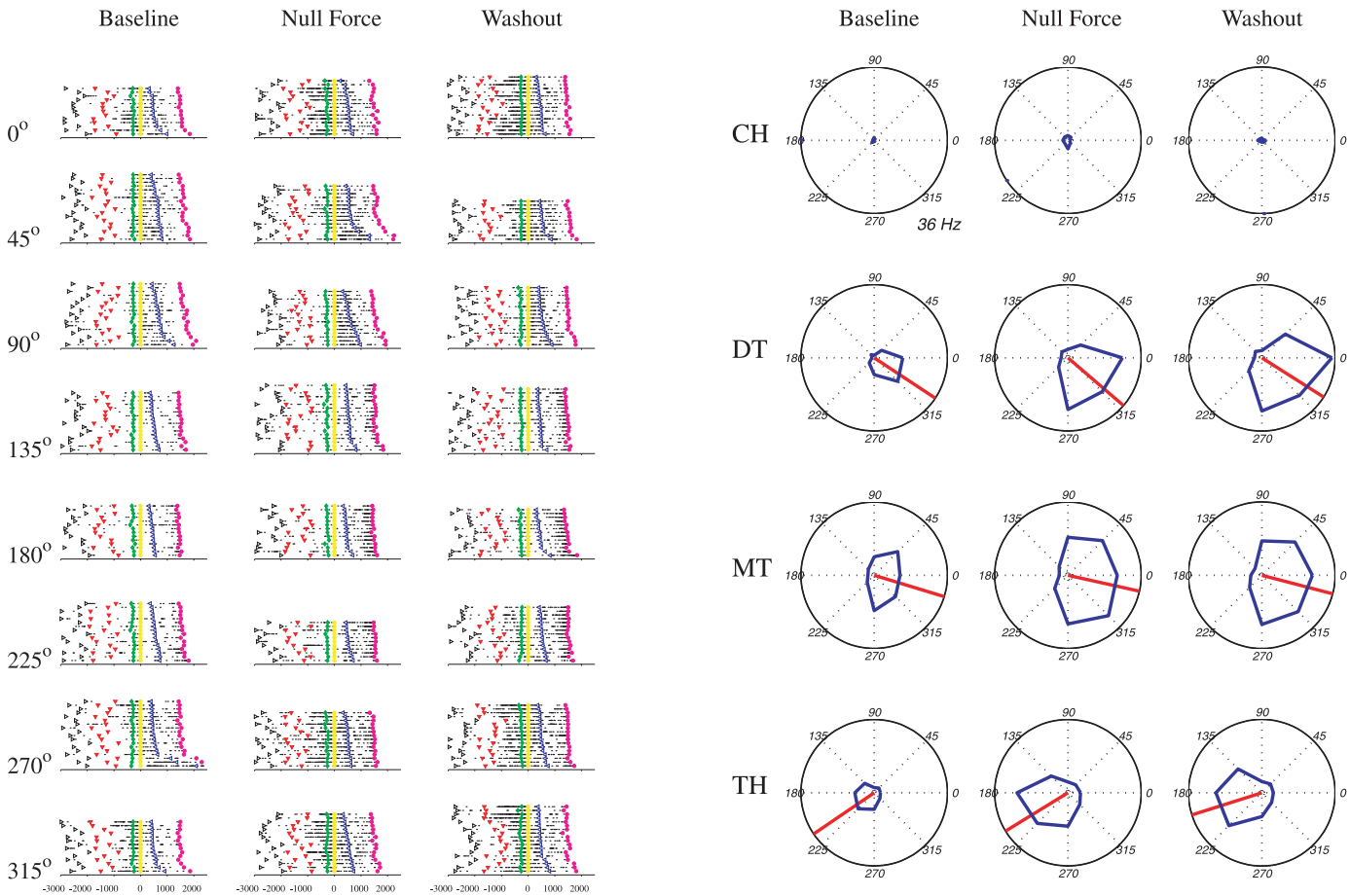

FIG. 13. A control cell. *Left*: raster plots. All conventions are as in Fig. 7. *Right*: this cell was recorded in a session where no perturbing force was ever introduced, and the monkey performed in BASELINE-like conditions throughout the session. Pd of the cell remained essentially unchanged throughout the 3 (arbitrarily defined) behavioral conditions, in the DT, MT, and TH time windows. Note, however, that the Avf of the cell increased over the course of the session. All conventions are as in Fig. 7.

highly predictive of each other. Considering the entire contingency table, we rejected the null hypothesis of homogeneity (Pearson's $\chi^2 = 104.94$, $df = 16$, $P < 10^{-14}$). Furthermore, the deviance from homogeneity was largely explained by the trace of the matrix $Tr = 62.27$, which indicated that the 2 classifications coincided more frequently than expected by chance ($df = 4$, $P < 10^{-12}$). The rest of the matrix, considered without the trace, did not indicate any further deviance from homogeneity.

We did not perform this analysis for the Tw because only 7 cells could be considered for the analysis.

Consistency of classification across time windows: MT and TH

Comparison of the MT and TH time windows provided similar results. With respect to the changes of Pd, analysis of the 5×5 contingency table did not provide evidence to reject the null hypothesis of homogeneity (Pearson's $\chi^2 = 13.34$, $df = 16$, $P = 0.6$). Likewise, analysis of the trace failed to indicate statistically significant coincidence of classification ($Tr = 1.45$, $df = 4$, $P = 0.8$).

In contrast, with respect to the changes of Avf, the classification in the MT and TH time windows were highly predictive of each other. The null hypothesis of homogeneity was rejected on the basis of the 5×5 contingency table (Pearson's $\chi^2 = 67.49$, $df = 16$, $P < 10^{-7}$), an effect largely explained by coincident classifications ($Tr = 31.22$, $df = 4$, $P < 10^{-5}$).

We did not perform this analysis for the Tw because only 10 cells could be considered for the analysis.

Consistency of classification across parameters

We also investigated whether the classification of cells was consistent across parameters. In general, we found that the classifications performed according to different parameters did not coincide more frequently than expected by chance. Considering the MT time window, we first combined the classification for the Pd with that for the Avf in a 5×5 contingency table. We then computed the matrix χ^2_{ij}. Analysis of the entire matrix failed to reject the null hypothesis of homogeneity (Pearson's $\chi^2 = 13.82$, $df = 16$, $P = 0.6$). Likewise, considering the trace Tr by itself revealed that the classification for the changes of Pd and that for the changes of Avf do not coincide more often than would be expected by chance ($Tr = 1.91$, $df = 4$, $P = 0.8$).

Because no cell was classified as "other" for its changes of Tw in the MT time window, we collapsed memory I, memory II, and other cells in a superclass of "memory" cells when considering the Tw in combination with either the Pd or the Avf. Combining the classification of the Pd with that of the Tw, we found no significant departure from homogeneity at the

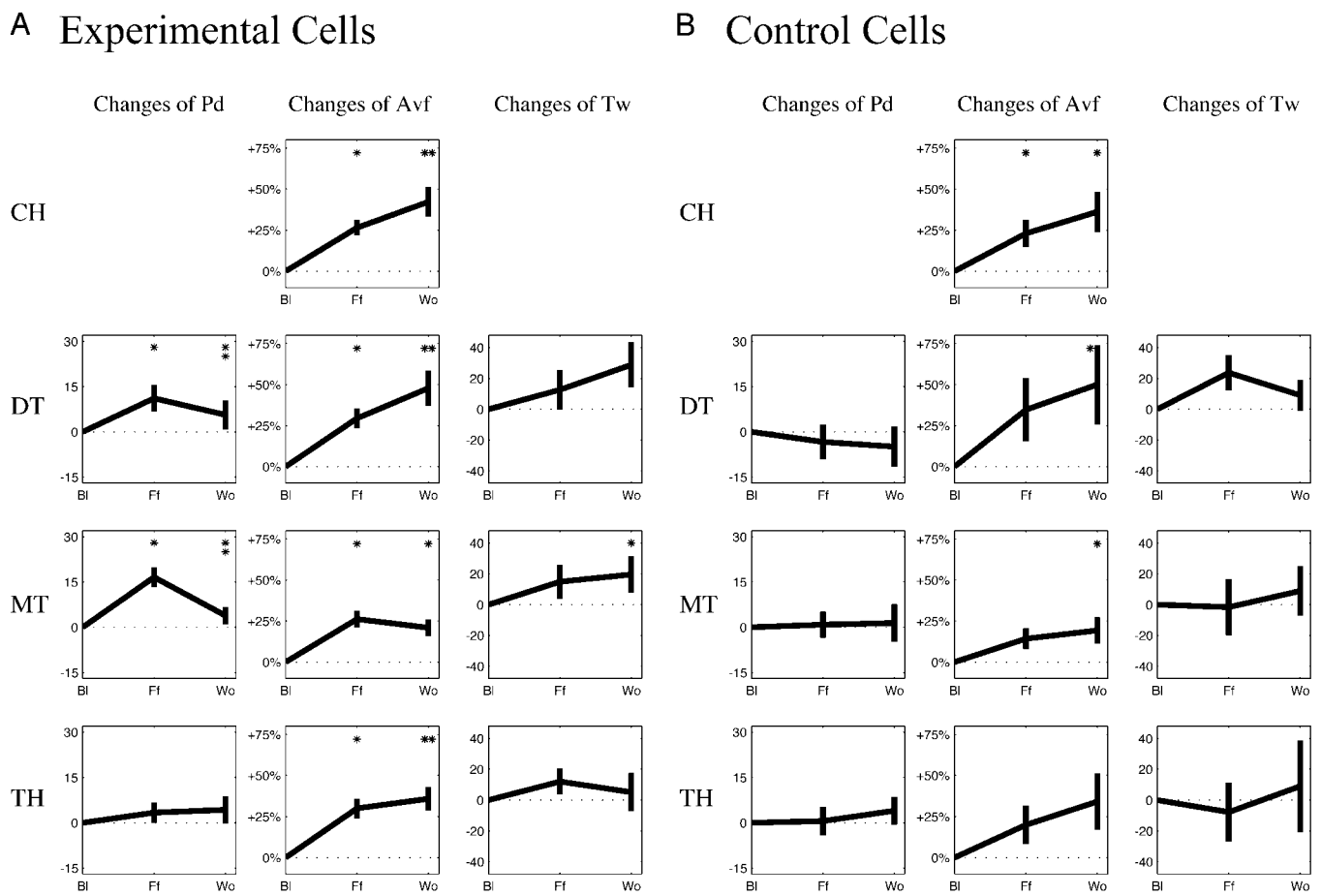

FIG. 14. Population changes. Summary of the changes observed at the population level for experimental cells (*A*, *left*) and for control cells (*B*, *right*), and for the 3 parameters preferred direction (Pd), average firing rate (Avf), and tuning width (Tw) (values in Table 3). *A*: experimental cells. Changes of Pd (*left column*). Consider first the DT (*top displayed panel*): the black line connects 3 data points, corresponding—on the *x*-axis—to the BASELINE (Bl), the FORCE condition (Ff), and the WASHOUT (Wo); the *y*-axis represents the shifts of Pd, where "zero" is the Pd in the BASELINE and positive values are shifts in the direction of the external force. Vertical lines indicate the error bars. In the DT, SMA neurons shifted their Pd in the FORCE condition compared with the BASELINE. Single asterisk indicates that this shift was significant. In the WASHOUT, SMA neurons shifted their Pd back in the opposite direction. The 2 vertically arranged asterisks indicate that the Pd in the WASHOUT was statistically the same as that in the BASELINE, but different from that in the FORCE condition. Similar shifts of Pd are observed in the MT. In contrast, no significant shifts of Pd are observed in the TH. Changes of Avf (*center column*). Consider the CH (*top panel*). Again, the *x*-axis corresponds to the 3 conditions (Bl, Ff, and Wo); the *y*-axis represents percentage changes of Avf compared with the BASELINE. Single asterisk indicates a significant increase of Avf in the FORCE compared with the BASELINE. Two horizontally arranged asterisks indicate that in the WASHOUT the Avf was significantly higher than that in both the FORCE condition and the BASELINE. Similar increases are observed in the DT, MT, and TH. In the MT, the increase of Avf in the WASHOUT does reach significance if compared with the BASELINE, but not if compared with the FORCE condition. Changes of Tw (*right column*). Here the *y*-axis represents increases in the Tw compared with the BASELINE. In general, we observe an increase of Tw in all 3 time windows. However, this increase reaches significance level only in the MT, when comparing the WASHOUT with the BASELINE (single asterisk). *B*: control cells. Format and conventions are the same as for experimental cells. At the population level, control cells show no significant shift of Pd and no significant change of Tw across conditions. In contrast, the Avf increases across conditions.

level of the entire matrix (Pearson's $\chi^2 = 4.09$, $df = 4$, $P = 0.4$), nor a significant coincidence considering the trace only ($Tr = 1.68$, $df = 2$, $P = 0.8$). Likewise, combining the classification of the Avf with that of the Tw, we found no significant departure from homogeneity at the level of the entire matrix (Pearson's $\chi^2 = 5.22$, $df = 4$, $P = 0.3$), nor a significant coincidence considering the trace only ($Tr = 2.30$, $df = 2$, $P = 0.7$).

Analysis of the reaction time (RT) and strictly-movement time (SMT) windows

In the present study, we analyzed the neuronal activity in 4 time windows: center hold (CH), delay time (DT), movement time (MT), and target hold time (TH). In particular, we defined MT as the time window starting 200 ms before the movement onset (*mo*) and ending at the end of movement (*me*). This definition was chosen for consistency with the previous analysis of neurons recorded in M1 (Li et al. 2001), and because studies that explicitly investigated this issue in M1 found minor differences between the activity recorded during the reaction time (RT; from the *go* to the *mo*), the strictly-movement time (SMT; from the *mo* to the *me*), and the combined time window (RT + SMT, roughly corresponding to the MT time window defined here) (Kalaska et al. 1989). In this section, we discuss the results of a control analysis of the activity of SMA neurons performed in the 2 separately defined time windows RT and SMT.

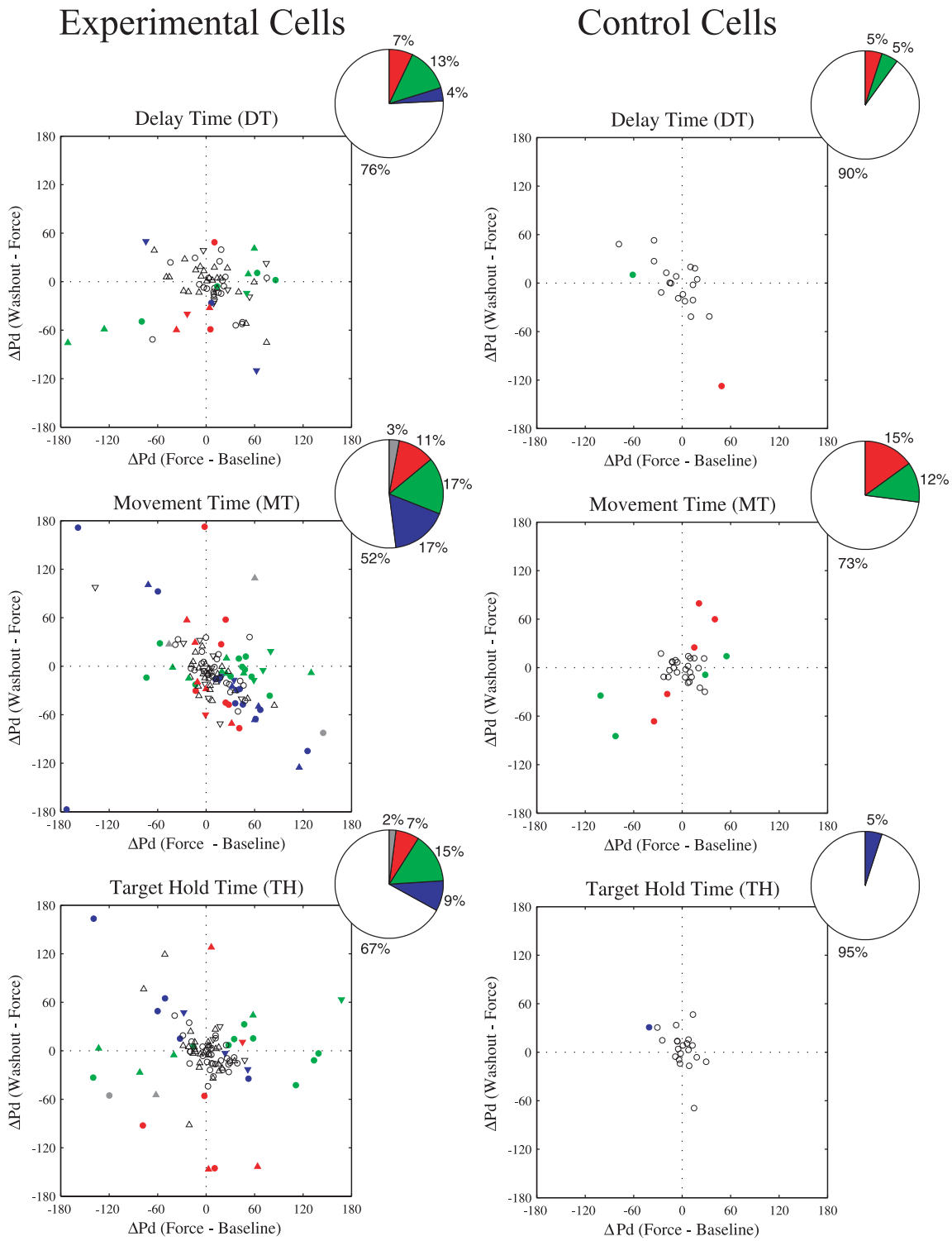

FIG. 15. Scatter plots: changes of Pd. Summary of the classification of neurons for their changes of Pd in the 3 time windows delay time (DT, *top*), movement time (MT, *center*), and target hold time (TH, *bottom*). Results are presented separately for experimental cells (*left column*) and for control cells (*right column*). In each plot, the *x*-axis represents the shift of Pd in the FORCE compared with BASELINE; the *y*-axis represents the shift of Pd in the WASHOUT compared with the FORCE. Positive values indicate shifts of Pd in the direction of the external force, and each data point represents one neuron. Colors indicate the result of the classification into kinematic cells (open symbols), dynamic cells (blue), memory I cells (green), memory II cells (red), and "other" cells (gray). Kinematic cells, which do not present significant shifts of Pd in either the FORCE or the WASHOUT, lie close to the axes origin. Dynamic cells, which present significant and opposite shift in the 2 measures, lie on the diagonal crossing the 2nd and 4th quadrants. Memory I and memory II cells, which present significant shifts of Pd in only one of the 2 measures, lie close to the *x*-axis and *y*-axis, respectively. For experimental cells, the different symbols refer to monkey F, CCK FORCE (inverted triangles); monkey C, CK FORCE (circles); and monkey C, CCK FORCE (triangles). Pie on the *upper right* of each plot summarizes the percentages of cells in each class.

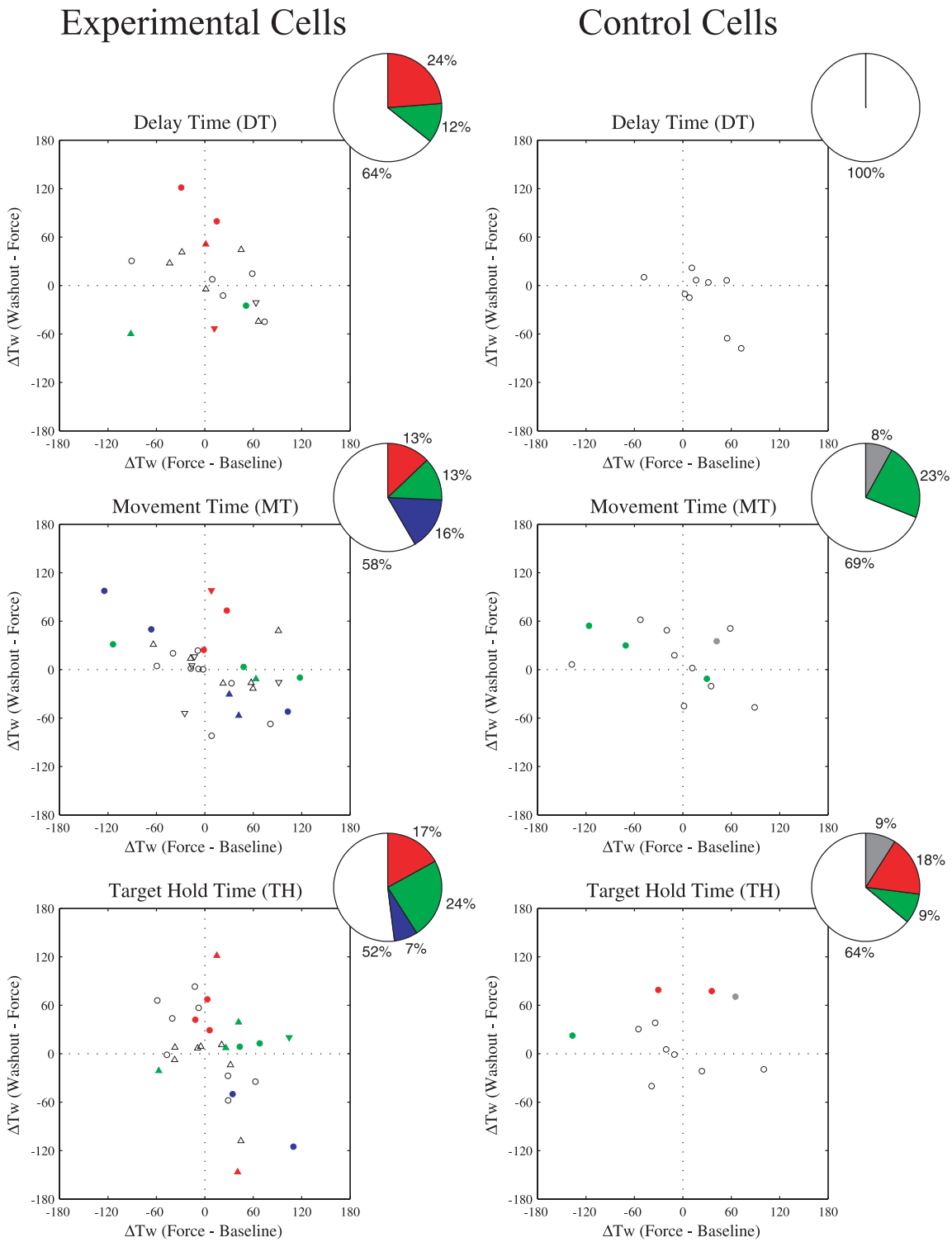

FIG. 16. Scatter plots: changes of tuning width (Tw). All conventions as in Fig. 15.

In total, we found that the BASELINE activity of 151 (60%) and 159 (63%) of cells was directionally tuned in the RT window and SMT window, respectively. For the FORCE condition, the corresponding numbers and percentages were 158 (63%) and 178 (71%) for RT and SMT, respectively. For the WASHOUT, the corresponding numbers and percentages were 154 (61%) and 166 (66%) for RT and SMT, respectively.

Considering the entire population, we recorded a significant shift of Pd in the direction of the external force in the FORCE condition compared with BASELINE both in the RT (9.11°; $P < 0.002$) and in the SMT (15.0°; $P < 0.001$) time windows. Comparing the WASHOUT and the FORCE conditions, the Pd shifted significantly in the opposite direction in both the RT (−5.6°; $P < 0.05$) and the SMT (−11.3°; $P < 0.003$) time windows. Finally, no significant shift of Pd was observed when comparing the WASHOUT and BASELINE in either the RT (5.7°;

$P = 0.1$) or the SMT (3.9°; $P = 0.2$) time window. In essence, these measures correspond well to the results previously described for the delay time (DT) and movement time (MT) windows.

Likewise with respect to the average firing frequency (Avf), the changes recorded in the RT and SMT time windows were similar to those previously observed in DT and MT. Specifically, the Avf increased significantly in both the RT and SMT time windows across conditions.

We also observed a general increase of the Tw across conditions. This increase, which was not significant in the RT time window (WASHOUT–BASELINE: mean increase of Tw = 19.6°; $P = 0.1$, circular *t*-test), did reach significance level in the SMT time window (WASHOUT–BASELINE: mean increase of Tw = 18.3°; $P < 0.03$, circular *t*-test). Again, these results for RT and SMT are essentially those expected from the previous analysis of the DT and MT time windows.

Finally, we analyzed neuronal plastic changes of Pd. The results for the RT and SMT time windows are illustrated in the scatter plots of Fig. 17 (experimental cells). Again, the results for the RT and SMT time windows are similar to those for the DT and MT time windows, respectively.

In conclusion, separate analysis of the RT and SMT time windows indicated a relatively smooth transition from values recorded in the DT to values recorded in the MT (as defined here) both for the population averages and for the percentages of cells found in each class. More specifically, we found minor differences between the results obtained for the strictly-movement–related time window (SMT) and the movement-related time window (MT) defined in this study.

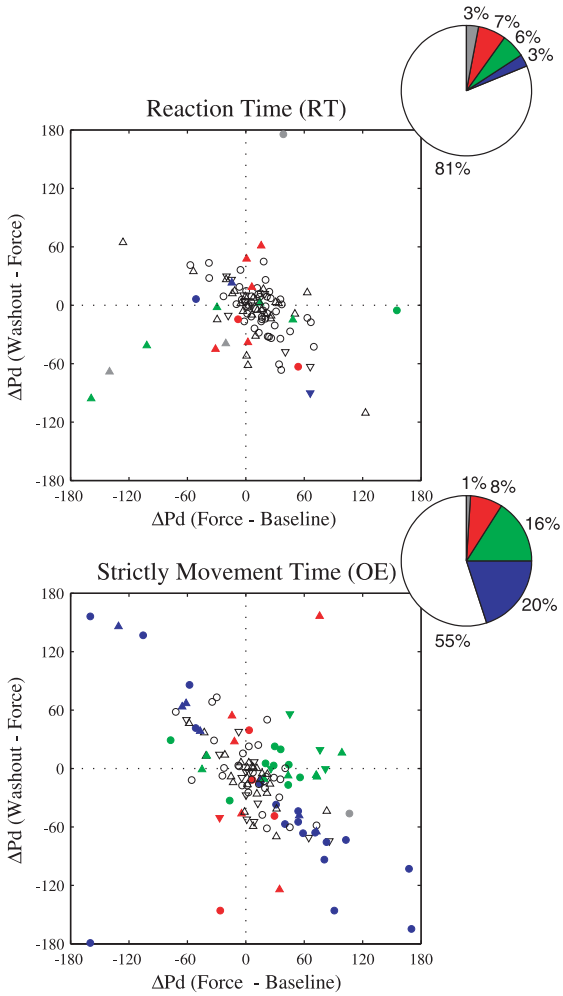

FIG. 17. Analysis of the RT and SMT time windows (shift of Pd, experimental cells). *Top scatter plot*: reaction time window (RT; from the *go* to the *mo*). *Bottom plot*: strictly-movement time window (SMT; from the *mo* to the *me*). All conventions as in Fig. 15.

DISCUSSION

In this study, we recorded and analyzed the activity of individual neurons in the supplementary motor area (SMA) before and during planar reaching movements. In particular, we investigated how their activity reflects the movement dynamics and how it modifies when monkeys adapt to perturbing force fields.

These experiments were conducted with two objectives. First, to further investigate how neurons in SMA participate to the processing of the movement dynamics. Second, to investigate whether and how neurons in SMA modify their activation patterns when monkeys acquire a new internal model for the dynamics, potentially contributing to this form of motor learning. With respect to the first issue, we used the shift of preferred direction (Pd) as a measure of dynamics-related activity. In essence, we found that, as a population, SMA neurons shifted their Pd in the direction of the external force when monkeys adapted to a perturbing force field, and back in the other direction when the monkeys readapted to the nonperturbed conditions. In contrast, no such shift was observed for the population of control cells, recorded with no perturbation. The population shift of Pd, observed during the instructed delay and during the movement-related time window, indicates that neurons in SMA do reflect the dynamics of the upcoming movement during movement planning and during movement execution.

With respect to the second issue—the contribution of SMA to motor learning—our conclusions are less definitive. On the one hand, when monkeys adapted to the external force and readapted to the nonperturbed conditions, neurons in SMA changed their activity patterns in a variety of ways consistent with learning, and similarly to what we had observed in M1 (Gandolfo et al. 2000; Li et al. 2001). On the other hand, our results relative to control cells are less clear-cut than we had expected.

Control cells were recorded in sessions in which no force was ever introduced and trials were arbitrarily divided in 3 "conditions" and were analyzed with the same procedure used for experimental cells. Comparing the results for the 2 populations at the level of individual neurons reveals that significant changes across conditions were more frequent among experimental cells than among control cells. Indeed, cells classified as kinematic for their changes of Pd in the MT time window were 73% for control cells versus 52% for experimental cells. This notwithstanding, we also report that a sizable percentage of control cells was classified—according to our criteria—as nonkinematic. For example, with respect to the changes of Pd in the MT time window, 4 (12%) and 5 (15%) control cells were classified as memory I and memory II, respectively. It is possible that these percentages partially reflect a statistical artifact attributed to the relatively small number of control cells (46 control cells vs. 252 experimental cells). Nonetheless, the

results obtained for control cells make the interpretation of experimental cells more complex.

One possibility is that the statistical criteria chosen to identify significant changes were too liberal and allowed to pick up noise. We actually do not think this is the case. The threshold for significant directional tuning was raised here to $P < 0.01$ from $P < 0.05$ used in the previous study on M1, and the threshold for significant changes across conditions was raised to $P < 0.001$ from $P < 0.01$. More important, inspection of the waveform and tuning curves of the 9 "memory" SMA control cells suggested to us that recordings were stable and the changes of Pd were "real." In any case, it can be excluded that all the changes of Pd observed here are attributed to random noise: if this were the case we would not observe the significant shift at the level of the population that we found for experimental cells but not for control cells.

We considered two alternative explanations. One possibility is that the changes of Pd observed for control cells are attributable to aspects of the task not fully controlled for, such as postural adjustments. This is a possibility even though we did not observe macroscopic postural changes during the experiments. Another possibility is that changes of Pd observed for control cells reflect a genuine long-term reorganization of the motor system. Previous work found extensive remapping in M1 after long-term motor practice (Elbert et al. 1995; Karni et al. 1998; Nudo et al. 1996; but see Plautz et al. 2000). Most interestingly in the present context, Tanji and colleagues found that extensive training of a simple key-press movement results in changed neuronal activation patterns in SMA (Aizawa et al. 1991). Such changes took place over 12 mo, much beyond the psychophysical task "learning" period of 2 mo. The present observation of memory properties for control cells is consistent with the idea that the nervous system continuously remodels itself as during learning, even at times where at the macroscopic and psychophysical level the monkey is not undergoing a learning experience. Thus changes recorded during control sessions could be related to continuing training of nonperturbed movements, similarly to that described by Aizawa et al. (1991). An alternative or complementary possibility is that changes recorded in control sessions (which were intermixed with experimental sessions) are partially related to the processes of consolidation following adaptation to a new force field (Brashers-Krug et al. 1996; see also Muellbacher et al. 2002; Shadmehr and Holcomb 1997).

Changes of average firing rate and tuning width

With respect to changes of average firing frequency (Avf), we recorded a general increase of Avf across conditions for both experimental and control cells in SMA, similarly to what we found for experimental cells in M1 (Li et al. 2001). One possible explanation of this increase is that the very presence of the electrode close to the neuron had an effect on the excitability over time. Alternatively, the increase in firing rate might also be the result of fatigue. Indeed, the effect was more pronounced for experimental cells, recorded when the monkey engaged in a presumably more effortful task. However, we lack a direct evidence for this hypothesis.

Experimental and control cells were also analyzed and classified for their changes of tuning width (Tw). For experimental cells, we often recorded significant changes of Tw across conditions. Similar changes were also recorded for control cells, although in relatively fewer cases. For example, in the DT time window, cells classified as kinematic with respect to the changes of Tw were 65% and 100% for the populations of experimental cells and control cells, respectively. The corresponding percentages for the MT time window were 59% and 69% for experimental cells and control cells, respectively. In this respect, the results for the Tw at the level of individual neurons offered a picture analogous to that emerging for the Pd.

Analysis of the population changes of Tw provided a somewhat intriguing result. At the population level, no changes were observed for control cells. In contrast, the Tw of experimental cells increased across conditions, an effect that became significant in the WASHOUT (MT time window). One possibility is that the broadening of the tuning curve recorded for experimental cells reflects in part the adaptation and readaptation experience and correlates with the acquisition of a new internal model for the dynamics.

Comparison with M1

One of the goals of this study was to compare the dynamics-related activity and plastic changes in SMA with that previously recorded in M1. One of the most interesting results was that neurons in SMA process the dynamics of the upcoming movement during the instructed delay, at a time when only few M1 neurons are directionally tuned and before dynamics-related activity can be recorded in M1. We have shown elsewhere that the activity of neurons in SMA comes to reflect the movement dynamics increasingly over the course of the delay, starting from a kinematics-related signal. This progressive shift, found for the population and for individual cells, suggests that neurons in SMA contribute to the processing of the kinematics-to-dynamics transformation (Padoa-Schioppa et al. 2002).

With respect to plastic changes, the present results should be compared with that for M1 but with some caveat. The statistical thresholds used here to define directional tuning ($P < 0.01$) and to identify significant changes of activity across conditions ($P < 0.001$) were more restrictive than those previously applied. We reanalyzed the data from M1. In particular, with respect to changes of Pd in the MT time window, classification of M1 cells according to the present criteria resulted in 26 (50%) kinematic, 9 (17%) dynamic, 8 (15%) memory I, and 9 (17%) memory II cells. A χ^2 analysis of the 2×5 contingency table failed to indicate significant differences between this classification for M1 and the corresponding results for SMA (Pearson's $\chi^2 = 2.49$, $df = 4$, $P = 0.6$). In other words, the plastic changes observed in SMA during and after adaptation to a new dynamic environment were qualitatively and quantitatively similar to those found in M1.

With respect to control cells, it should be noticed that only 7 control cells were recorded in M1. The 3 neurons that could be analyzed for their changes of Pd in the MT time window were all classified as kinematic cells. Although the number is too small to conclude that M1 control cells do not change their activity patterns across conditions, we do not think that the results found for SMA control cells can be directly translated to interpret M1 experimental cells. In fact, it is possible that long-term changes related to continuing training, similarly to

that described by Tanji and colleagues, are characteristic of SMA (Aizawa et al. 1991). Thus we think that the evidence from our experiments, together with results described in an increasingly rich literature (Classen et al. 1998; Karni et al. 1995; Laubach et al. 2000; Muellbacher et al. 2002; Rioult-Pedotti et al. 1998; Sanes and Donoghue 2000; Shadmehr and Holcomb 1997; Wise et al. 1998), argues for an involvement of M1 in general in motor learning, and in particular in the acquisition of a new internal model for the dynamics. The issues raised for SMA by control cells remain open questions for M1 and should be addressed by new recordings.

Interpretative concerns

In this series of studies, we interpret the activity of neurons that does not change after adaptation to the force and readaptation to the nonperturbed conditions as related to the movement kinematics. Activity that does change we interpret as related to the movement dynamics. These interpretations need some clarification.

First, from a statistical standpoint, the inclusion of a neuron in the kinematic class is a weak statement because it corresponds to the null hypothesis. In other words, it is likely that some of the cells classified as kinematic really coded for aspects of the dynamics. Second, the movement kinematics was not the only variable that remained unchanged across conditions. Other force-independent variables include any sensory or cognitive process "upstream" of the desired kinematics, and presumably variables related to the eye position (which we did not record). It is likely that at least some of these variables modulated the activity of neurons described here. Nonetheless, as we have previously argued (Padoa-Schioppa et al. 2002), it is likely that neurons recorded here, particularly when their activity did not change across conditions, did *also* code for aspects of the desired kinematics, under the understanding that desired kinematics is the last processing stage before the movement dynamics (Alexander and Crutcher 1990b; Kakei et al. 1999; Kalaska and Crammond 1992; Mussa-Ivaldi and Bizzi 2000; Saltzman 1979; Shadmehr and Mussa-Ivaldi 1994; Wolpert and Ghahramani 2000).

Another possible concern relates to the fact that the actual kinematics did in fact partly change across conditions because the convergence trends corresponding to the processes of adaptation and long-term learning were not always complete within the recording trials and sessions. However, as we noted above (RESULTS) the convergence trend observed for the actual kinematics suggests that the desired kinematics was unchanged across conditions. In addition, it should be noted that the preferred direction of a neuron that reflected the actual kinematics would shift, because of incomplete adaptation, in the direction opposite to the direction of the external force. This contrasts with our findings. Thus changes in neuronal activity recorded here cannot easily be explained by the fact that adaptation was not completed within the span of our recordings.

In conclusion, our results confirm that neurons in SMA participate in the processing of the movement dynamics during motor preparation and execution. With respect to plastic changes associated with learning of a new dynamics, comparison of the results for experimental SMA cells with those for control SMA cells provides a more complex picture than we had expected after our experiment on M1. This notwithstanding, the present results are consistent with the hypothesis that neurons in SMA play a role in the acquisition of a new internal model of the dynamics, as neurons in M1 do.

DISCLOSURES

This research was supported by National Institute of Mental Health Grant MH-48185.

Present addresses: C. Padoa-Schioppa, Department of Neurobiology, Harvard Medical School, 200 Longwood Ave., Boston, MA 02115; C.-S.R. Li, Psychiatry Service 116A, Yale University/VA Medical Center, 950 Campbell Ave., West Haven, CT 06516.

REFERENCES

Aizawa H, Inase M, Mushiake H, Shima K, and Tanji J. Reorganization of activity in the supplementary motor area associated with motor learning and functional recovery. *Exp Brain Res* 84: 668–671, 1991.

Alexander GE and Crutcher MD. Neural representations of the target (goal) of visually guided arm movements in three motor areas of the monkey. *J Neurophysiol* 64: 164–178, 1990a.

Alexander GE and Crutcher MD. Preparation for movement: neural representations of intended direction in three motor areas of the monkey. *J Neurophysiol* 64: 133–150, 1990b.

Bates JF and Goldman-Rakic PS. Prefrontal connections of medial motor areas in the rhesus monkey. *J Comp Neurol* 336: 211–228, 1993.

Bernstein NA. *The Co-ordination and Regulation of Movements.* New York: Pergamon Press, 1967.

Brashers-Krug T, Shadmehr R, and Bizzi E. Consolidation in human motor memory. *Nature* 382: 252–255, 1996.

Cadoret G and Smith AM. Comparison of the neuronal activity in the SMA and the ventral cingulate cortex during prehension in the monkey. *J Neurophysiol* 77: 153–166, 1997.

Chen LL and Wise SP. Neuronal activity in the supplementary eye field during acquisition of conditional oculomotor associations. *J Neurophysiol* 73: 1101–1121, 1995.

Classen J, Liepert J, Wise SP, Hallett M, and Cohen LG. Rapid plasticity of human cortical movement representation induced by practice. *J Neurophysiol* 79: 1117–1123, 1998.

Crutcher MD and Alexander GE. Movement-related neuronal activity selectively coding either direction or muscle pattern in three motor areas of the monkey. *J Neurophysiol* 64: 151–163, 1990.

Desmurget M and Grafton S. Forward modeling allows feedback control for fast reaching movements. *Trends Cogn Sci* 4: 423–431, 2000.

Dum RP and Strick PL. The origin of corticospinal projections from the premotor areas in the frontal lobe. *J Neurosci* 11: 667–689, 1991.

Elbert T, Pantev C, Wienbruch C, Rockstroh B, and Taub E. Increased cortical representation of the fingers of the left hand in string players. *Science* 270: 305–307, 1995.

Evarts EV. Relation of pyramidal tract activity to force exerted during voluntary movement. *J Neurophysiol* 31: 14–27, 1968.

Fisher NI. *Statistical Analysis of Circular Data.* New York: Cambridge Univ. Press, 1993.

Flanagan JR, Nakano E, Imamizu H, Osu R, Yoshioka T, and Kawato M. Composition and decomposition of internal models in motor learning under altered kinematic and dynamic environments. *J Neurosci* 19: RC34, 1999.

Freeman DH. *Applied Categorical Data Analysis.* New York: Marcel Dekker, 1987.

Gandolfo F, Li C, Benda BJ, Padoa-Schioppa C, and Bizzi E. Cortical correlates of learning in monkeys adapting to a new dynamical environment. *Proc Natl Acad Sci USA* 97: 2259–2263, 2000.

Geyer S, Matelli M, Luppino G, and Zilles K. Functional neuroanatomy of the primate isocortical motor system. *Anat Embryol* (*Berl*) 202: 443–474, 2000.

Halsband U, Matsuzaka Y, and Tanji J. Neuronal activity in the primate supplementary, pre-supplementary and premotor cortex during externally and internally instructed sequential movements. *Neurosci Res* 20: 149–155, 1994.

He SQ, Dum RP, and Strick PL. Topographic organization of corticospinal projections from the frontal lobe: motor areas on the lateral surface of the hemisphere. *J Neurosci* 13: 952–980, 1993.

He SQ, Dum RP, and Strick PL. Topographic organization of corticospinal projections from the frontal lobe: motor areas on the medial surface of the hemisphere. *J Neurosci* 15: 3284–3306, 1995.

Hikosaka O, Sakai K, Nakahara H, Lu S, Miyachi S, Nakamura K, and Rand MK. *The New Cognitive Neuroscience*, edited by Gazzaniga MS. Cambridge, MA: MIT Press, 2000, p. 553–572.

Kakei S, Hoffman DS, and Strick PL. Muscle and movement representations in the primary motor cortex. *Science* 285: 2136–2139, 1999.

Kalaska JF, Cohen DA, Hyde ML, and Prud'homme M. A comparison of movement direction-related versus load direction-related activity in primate motor cortex, using a two-dimensional reaching task. *J Neurosci* 9: 2080–2102, 1989.

Kalaska JF and Crammond DJ. Cerebral cortical mechanisms of reaching movements. *Science* 255: 1517–1523, 1992.

Karni A, Meyer G, Jezzard P, Adams MM, Turner R, and Ungerleider LG. Functional MRI evidence for adult motor cortex plasticity during motor skill learning. *Nature* 377: 155–158, 1995.

Karni A, Meyer G, Rey-Hipolito C, Jezzard P, Adams MM, Turner R, and Ungerleider LG. The acquisition of skilled motor performance: fast and slow experience-driven changes in primary motor cortex. *Proc Natl Acad Sci USA* 95: 861–868, 1998.

Kawato M. Internal models for motor control and trajectory planning. *Curr Opin Neurobiol* 9: 718–727, 1999.

Krakauer JW, Ghilardi MF, and Ghez C. Independent learning of internal models for kinematic and dynamic control of reaching. *Nat Neurosci* 2: 1026–1031, 1999.

Kurata K and Tanji J. Contrasting neuronal activity in supplementary and precentral motor cortex of monkeys. II. Responses to movement triggering vs. nontriggering sensory signals. *J Neurophysiol* 53: 142–152, 1985.

Laubach M, Wessberg J, and Nicolelis MA. Cortical ensemble activity increasingly predicts behaviour outcomes during learning of a motor task. *Nature* 405: 567–571, 2000.

Li CS, Padoa-Schioppa C, and Bizzi E. Neuronal correlates of motor performance and motor learning in the primary motor cortex of monkeys adapting to an external force field. *Neuron* 30: 593–607, 2001.

Luppino G, Matelli M, Camarda RM, Gallese V, and Rizzolatti G. Multiple representations of body movements in mesial area 6 and the adjacent cingulate cortex: an intracortical microstimulation study in the macaque monkey. *J Comp Neurol* 311: 463–482, 1991.

Luppino G, Matelli M, Camarda R, and Rizzolatti G. Corticocortical connections of area F3 (SMA-proper) and area F6 (pre-SMA) in the macaque monkey. *J Comp Neurol* 338: 114–140, 1993.

Luppino G, Matelli M, Camarda R, and Rizzolatti G. Corticospinal projections from mesial frontal and cingulate areas in the monkey. *Neuroreport* 5: 2545–2548, 1994.

Luppino G, Matelli M, and Rizzolatti G. Cortico-cortical connections of two electrophysiologically identified arm representations in the mesial agranular frontal cortex. *Exp Brain Res* 82: 214–218, 1990.

Matelli M, Luppino G, and Rizzolatti G. Architecture of superior and mesial area 6 and the adjacent cingulate cortex in the macaque monkey. *J Comp Neurol* 311: 445–462, 1991.

Matsuzaka Y, Aizawa H, and Tanji J. A motor area rostral to the supplementary motor area (presupplementary motor area) in the monkey: neuronal activity during a learned motor task. *J Neurophysiol* 68: 653–662, 1992.

Matsuzaka Y and Tanji J. Changing directions of forthcoming arm movements: neuronal activity in the presupplementary and supplementary motor area of monkey cerebral cortex. *J Neurophysiol* 76: 2327–2342, 1996.

Merfeld DM, Zupan L, and Peterka RJ. Humans use internal models to estimate gravity and linear acceleration. *Nature* 398: 615–618, 1999.

Muellbacher W, Ziemann U, Wissel J, Dang N, Kofler M, Facchini S, Boroojerdi B, Poewe W, and Hallett M. Early consolidation in human primary motor cortex. *Nature* 415: 640–644, 2002.

Mushiake H, Inase M, and Tanji J. Neuronal activity in the primate premotor, supplementary, and precentral motor cortex during visually guided and internally determined sequential movements. *J Neurophysiol* 66: 705–718, 1991.

Mussa-Ivaldi FA and Bizzi E. Motor learning through the combination of primitives. *Philos Trans R Soc Lond B Biol Sci* 355: 1755–1769, 2000.

Nakamura K, Sakai K, and Hikosaka O. Neuronal activity in medial frontal cortex during learning of sequential procedures. *J Neurophysiol* 80: 2671–2687, 1998.

Nudo RJ, Milliken GW, Jenkins WM, and Merzenich MM. Use-dependent alterations of movement representations in primary motor cortex of adult squirrel monkeys. *J Neurosci* 16: 785–807, 1996.

Okano K and Tanji J. Neuronal activities in the primate motor fields of the agranular frontal cortex preceding visually triggered and self-paced movement. *Exp Brain Res* 66: 155–166, 1987.

Padoa-Schioppa C, Li CS, and Bizzi E. Neural activity in the supplementary motor area during delayed reaching movements and adaptation to an external force field. *Soc Neurosci Abstr* 26: 590.4, 2000.

Padoa-Schioppa C, Li CS, and Bizzi E. Neuronal correlates of kinematics-to-dynamics transformation in the supplementary motor area. *Neuron* 36: 751–765, 2002.

Penfield W and Welch K. The supplementary motor area of the cerebral cortex. *Arch Neurol Psychiatry* 66: 289–317, 1951.

Picard N and Strick PL. Motor areas of the medial wall: a review of their location and functional activation. *Cereb Cortex* 6: 342–353, 1996.

Picard N and Strick PL. Imaging the premotor areas. *Curr Opin Neurobiol* 11: 663–672, 2001.

Plautz EJ, Milliken GW, and Nudo RJ. Effects of repetitive motor training on movement representations in adult squirrel monkeys: role of use versus learning. *Neurobiol Learn Mem* 74: 27–55, 2000.

Prut Y and Fetz EE. Primate spinal interneurons show pre-movement instructed delay activity. *Nature* 401: 590–594, 1999.

Rioult-Pedotti MS, Friedman D, Hess G, and Donoghue JP. Strengthening of horizontal cortical connections following skill learning. *Nat Neurosci* 1: 230–234, 1998.

Rouiller EM, Moret V, Tanne J, and Boussaoud D. Evidence for direct connections between the hand region of the supplementary motor area and cervical motoneurons in the macaque monkey. *Eur J Neurosci* 8: 1055–1059, 1996.

Saltzman E. Levels of sensorimotor representation. *J Math Psychol* 20: 91–163, 1979.

Sanes JN and Donoghue JP. Plasticity and primary motor cortex. *Annu Rev Neurosci* 23: 393–415, 2000.

Scott SH and Kalaska JF. Reaching movements with similar hand paths but different arm orientations. I. Activity of individual cells in motor cortex. *J Neurophysiol* 77: 826–852, 1997.

Scott SH, Sergio LE, and Kalaska JF. Reaching movements with similar hand paths but different arm orientations. II. Activity of individual cells in dorsal premotor cortex and parietal area 5. *J Neurophysiol* 78: 2413–2426, 1997.

Shadmehr R and Holcomb HH. Neural correlates of motor memory consolidation. *Science* 277: 821–825, 1997.

Shadmehr R and Moussavi ZM. Spatial generalization from learning dynamics of reaching movements. *J Neurosci* 20: 7807–7815, 2000.

Shadmehr R and Mussa-Ivaldi FA. Adaptive representation of dynamics during learning of a motor task. *J Neurosci* 14: 3208–3224, 1994.

Tanji J and Kurata K. Contrasting neuronal activity in supplementary and precentral motor cortex of monkeys. I. Responses to instructions determining motor responses to forthcoming signals of different modalities. *J Neurophysiol* 53: 129–141, 1985.

Tanji J, Taniguchi K, and Saga T. Supplementary motor area: neuronal response to motor instructions. *J Neurophysiol* 43: 60–68, 1980.

Thaler D, Chen YC, Nixon PD, Stern CE, and Passingham RE. The functions of the medial premotor cortex. I. Simple learned movements. *Exp Brain Res* 102: 445–460, 1995.

Thoroughman KA and Shadmehr R. Electromyographic correlates of learning an internal model of reaching movements. *J Neurosci* 19: 8573–8588, 1999.

Thoroughman KA and Shadmehr R. Learning of action through adaptive combination of motor primitives. *Nature* 407: 742–747, 2000.

Wise SP, Moody SL, Blomstrom KJ, and Mitz AR. Changes in motor cortical activity during visuomotor adaptation. *Exp Brain Res* 121: 285–299, 1998.

Wolpert DM and Ghahramani Z. Computational principles of movement neuroscience. *Nat Neurosci Suppl* 3: 1212–1217, 2000.

Wolpert DM, Ghahramani Z, and Jordan MI. An internal model for sensorimotor integration. *Science* 269: 1880–1882, 1995.

Woolsey CN, Settlage PH, Meyer DR, Sencer W, Pinto Hamuly T, and Travis AM. Patterns of localization in precentral and "supplementary" motor areas and their relation to the concept of premotor area. *Res Publ Assoc Nerv Ment Dis* 30: 231–250, 1952.